An innovative approach to solve the carsharing demand-supply imbalance problem under demand uncertainty

Huang, Kai; An, Kun; Correia, Gonçalo Homem de Almeida; Rich, Jeppe; Ma, Wanjing

DOI
10.1016/j.trc.2021.103369

Publication date
2021

Document Version
Accepted author manuscript

Published in
Transportation Research Part C: Emerging Technologies

Citation (APA)
Huang, K., An, K., Correia, G. H. D. A., Rich, J., & Ma, W. (2021). An innovative approach to solve the carsharing demand-supply imbalance problem under demand uncertainty. *Transportation Research Part C: Emerging Technologies*, *132*, Article 103369. https://doi.org/10.1016/j.trc.2021.103369

An Innovative Approach to Solve the Carsharing Demand-supply Imbalance Problem under Demand Uncertainty

Kai Huang[1, 2], Kun An[1, 2]*, Gonçalo Homem de Almeida Correia[3], Jeppe Rich[4], Wanjing Ma[1]
[1]College of Transportation Engineering, Tongji University, 4800 Cao'an Road, Shanghai, China
[2]Institute of Transport Studies, Department of Civil Engineering, Monash University, Melbourne, Australia
[3]Department of Transport & Planning, Delft University of Technology, Delft, the Nederlands
[4]Department of Management, Technical University of Denmark, Denmark
*Email: kunan@tongji.edu.cn

Abstract

This paper studies the demand-supply imbalance problem for one-way carsharing systems under a combination of pricing strategy, relocations and access trips considering stochastic demand. A novel concept of a virtual zone is utilized to capture vehicle relocation range and client walking or biking distance constraints in one-way carsharing systems. The vehicle imbalance problem is further addressed by combining a long-term pricing strategy and real-time vehicle relocations in a two-stage stochastic programming model. In the first stage, the tactical decisions including fleet size and trip price are optimized, while anticipating the operational costs from the second stage. The second stage optimizes operational decisions under uncertain demand including vehicle relocations conditional on the tactical decisions in stage one. The model aims to maximize the profit of a carsharing company considering the fleet costs calculated in stage one and the expected operational costs and revenue obtained in stage two. A dedicated gradient search algorithm is developed to solve the two-stage stochastic programming and results are compared to a genetic algorithm and an iterated local search algorithm. The proposed model and corresponding solution approach are applied to a large-scale network with 50 zones and over 1000 vehicles in Suzhou, China. The application allows us to attain additional operational insight. Results suggest that increased prices for high demand stations during peak hours reduce demand while maintaining profitability of the system. It is also found that the real-time vehicle relocations and flexibility of clients to pick up vehicles at farther stations can increase demand service rate by as much as 10%.

Keywords: One-way carsharing; Stochastic demand; Imbalance problem; Transport pricing; Vehicle relocation; Access trip

1 Introduction

In recent years, one-way carsharing has received increasing attention in both industry and academia. Many conventional car rental companies and Transport Network Companies have started to provide one-way carsharing services. For example, EVCARD in China owns 50,000 electric vehicles and 13,000 parking stations in 65 cities, enabling over 1,840,000 trips per month (EVCARD, 2021). ShareNow, which is the result of a merge between Car2go and DriveNow, is now offered in many cities all over the world. Zhou et al. (2017) forecasted that the carsharing market is expected to increase to 11%-25% of all trips in Australia, Indonesia, Malaysia, and Thailand in 2030. Many existing studies anticipate that carsharing will become one of the main travel modes in the next decades (Shaheen, 2006; Zheng et al., 2009; Shaheen and Cohen, 2013; Catalano et al., 2018).

Research with respect to one-way carsharing system design has mainly focused on three categories of decisions: strategic, tactical, and operational. The location, number, and capacity of carsharing stations are regarded as strategic decisions that should be fixed over a long period of time. Tactical decisions include fleet size and trip price, which typically are more flexible to modify than strategic decisions. The vehicle and personnel relocations fall under the category of operational decisions, which can change from day to day to be in line with actual demand (Boyacı et al., 2015; Xu et al., 2018). Due to inherent demand uncertainty, the number of trip requests at a station varies by the hour, day and week (An and Lo, 2014; 2015; 2016). It is therefore challenging to jointly optimize the long-term strategic/tactical decisions and the real-time operation decisions considering uncertainty in demand.

Existing studies usually assume deterministic demand with given origins and destinations (Di Febbraro et al., 2012; Barrios and Godier, 2014; Dandl and Bogenberger, 2018; Balac et al., 2019; Xu and Meng, 2019). A few studies also addressed demand elasticity where the demand for carsharing changes with the supply. Huang et al. (2018) used a logit model to estimate the proportion of people choosing carsharing compared to the other modes. Jorge et al. (2015) and Xu et al. (2018) built a price-based elastic demand function to predict the carsharing demand. All the above studies assumed deterministic demand over a period of time when optimizing the strategic or tactical decisions including station location, station capacity, and trip price. However, such results may lead to substantial losses or disturbances in the level of service during operation when demand is uncertain. How to make long-term decisions in order to maximize the expected profit while taking stochastic demand into account hereby becomes a relevant and challenging objective. Biondi et al. (2016), Brandstätter et al. (2017) and Fan (2014) optimized the strategic planning, including charging station locations, parking station locations and vehicle allocation, of carsharing system by exploring several different demand scenarios. Lu et al. (2018) studied a strategic planning problem by optimizing the number of parking lots and fleet size under demand uncertainty. The authors built a novel spatial-temporal network to capture vehicle flows between stations at different time steps. A two-stage stochastic integer programming model is formulated to address demand uncertainty in carsharing systems. Li et al. (2019) explored the imbalance problem between vehicle supply and carsharing demand under uncertain demand. Different from the above stochastic programming approach, He et al. (2017, 2020) adopted robust optimization to address demand uncertainty in the carsharing service region design problem.

One notorious difficulty in one-way carsharing operation arises from its inherent demand-supply imbalance problem. The carsharing operator has to relocate vehicles from stations with excess supply to with excess demand. Weikl and Bogenberger (2015) proposed a two-level zoning approach to handle vehicle relocations. To mitigate the computation burden, they divided the study region into several macroscopic zones with each macroscopic zone consisting of several microscopic zones. Vehicle relocations are then separated into those that travel between macroscopic zones and within macroscopic zones. Santos and Correia (2019) built a simulation-based optimization model to explore vehicle relocations with a real-time decision support tool where movements of staff necessary to relocate and maintain vehicles are modeled in details. Boyacı et al. (2017; 2019) proposed a time augmented network to optimize personnel movements before and after relocations. The relocation is carried out by hired drivers, either trip-based or full-time employed and is commonly referred to as operator-based vehicle relocation (Herbawi et al., 2016).

In comparison, pricing is another method to address the imbalance problem. In practice, a low vehicle rental price in high supply zones encourages users to drive vehicles to high demand zones (Di Febbraro et al., 2012, Jorge et al., 2015; He et al., 2019; Lu et al., 2020). Since people are usually less sensitive to short-term price changes, the pricing method is more suitable to affect people's demand if the price is relatively stable. In other words, decreasing the price from \$60/hour at 9 am to \$30/hour at 10 am on a random day is not likely to increase the demand much at 10 am on that day. However, if we fix the price as low as \$30/hour at 10 am for a whole year, the demand is more likely to increase and eventually become stable. Please note that the pricing method is not equivalent to the user-based vehicle relocation method. Pricing method is to decide the magnitude of demand, while user-based relocation aims to modify clients' behavior by payment discounts based on the given pricing strategy (Schiffer et al., 2021).

Different from the existing user-based relocation methods including trip-joining, trip-splitting, trip-based payment discounting and station-based payment discount (Barth et al., 2004; Uesugi et al., 2007; Huang et al., 2020a), users' behavior in choosing the pick-up or drop-off station also significantly affects the demand pattern and the performance of the carsharing system. Users may have to rent vehicles in neighboring stations within a certain maximum access distance if there are no vehicles available at the closest desired origin station (Boyacı et al., 2015). This uncertainty in pick-up location caused by vehicles' depletion adds to the difficulties in managing carsharing systems operations. Some studies capture this problem by tracking the complete trip chain of clients. Users can walk or bike from their origin to pick up their vehicles. A carsharing trip thus consists of two trip segments: access trip, and in-vehicle trip. Agent-based simulation can be used to track clients' status including walking, driving, and other activities during the rental period. Several authors use agent-based modeling such as MATSIM or models specifically built to study carsharing operations and impacts (Ciari et al., 2015; Heilig et al., 2018., Martínez et al., 2017; Vasconcelos et al., 2017). Despite its realism, the simulation approach makes it difficult to search for optimal policies when managing carsharing systems. Only a limited number of studies use mathematical formulations to model users' flexible pick-up locations allowing access trips. In order to model the access trip, one has to define the service radius or maximum access distance (Correia et al., 2014; Huang et al., 2018; Molnar and Correia, 2019). Cocca et al. (2019) found that a sizeable number of clients have the access distance between 1.4 km and 2.5 km from their desired origin/destination to a carsharing station. Brandstätter et al. (2017) put forward an interval for walking time that should be between 5 and 10 minutes in accessing or returning a vehicle to maintain a high level of service satisfaction.

In summary, the pricing problem and users' flexible pick-up station behavior under demand uncertainty make it challenging to solve the vehicle-demand imbalance problem. Three key issues need to be addressed: (i) set up tactical decisions including trip price with uncertain demand; (ii) tackle the imbalance problem between available vehicles and demand considering the fluctuations of daily carsharing requests; (iii) allow the flexible pick-up stations for users subject to car availability. Table 1 summarizes the cited literatures in vehicle-demand imbalance and demand uncertainty problems. To the authors' best knowledge, this paper is the first one to use such a method to address the imbalance problem.

Table 1 Summary the cited literatures in vehicle-demand imbalance and demand uncertainty problems

Literature	Vehicle-demand imbalance problem			Demand uncertainty	
	Rebalancing with flexible pricing	Relocation with hired drivers	Users' access trips	Stochastic programming	Robust optimization
Balac et al. (2019)		×			
Barrios and Godier (2014)		×			
Barth et al. (2004)	×				
Biondi et al. (2016)		×		×	
Boyacı et al. (2015)		×	×		
Boyacı et al. (2017)		×			
Boyacı et al. (2019)		×			

Brandstätter et al. (2017)			×	×		
Correia et al. (2014)		×	×			
Ciari et al. (2015)			×			
Cocca et al. (2019)			×			
Di Febbraro et al. (2012)	×					
Dandl and Bogenberger (2018)		×				
Fan (2014)		×		×		
Folkestad et al. (2020)		×				
He et al. (2020)		×				×
He et al. (2017)		×				×
Huang et al. (2018)		×				
Huang et al. (2020a)		×				
Huang et al. (2020b)	×	×				
Herbawi et al. (2016)		×				
Heilig et al. (2018)			×			
Jorge et al. (2015)	×	×				
Lu et al. (2018)		×		×		
Lu et al. (2020)	×	×				
Li et al. (2019)		×		×		
Molnar and Correia (2019)		×	×			
Santos and Correia (2019)		×				
Schiffer et al. (2021)	×					
Vasconcelos et al. (2017)		×	×			
Weikl and Bogenberger (2015)		×				
Xu et al. (2018)	×	×				
Xu and Meng (2019)		×				

Sample Average Approximation (SAA) is typically adopted to handle stochastic programming models, which can be solved by using commercial software such as Gurobi or CPLEX, the L-shaped method (Laporte and Louveaux, 1993), or the proposed service reliability-based gradient search algorithm (An and Lo, 2014). The gradient search algorithm has the advantages of addressing large-size network with similar size of stage-1 and stage-2 problems across different iterations and speeding up the algorithm with warm start.

In this paper, we propose an innovative approach, which consists of long-term pricing, real-time relocations and access trips for vehicle pick-up, to solve the demand-supply imbalance problem in one-way carsharing systems considering demand uncertainty. A Mixed-integer Non-linear Programming (MINLP) model is proposed to solve the problem. We assume that the carsharing operator aims to maximize the total profits by deciding the price, fleet size, and vehicle relocations. To address the stochasticity of demand, a two-stage formulation is developed where the novel notion of demand service rate is introduced to iterate between the two stages. Stage-1 determines the tactical decisions including the fleet size and trip price based on a given service rate. Stage-2 optimizes vehicle relocations considering stochastic demand. Pricing in Stage-1 determines the expected demand for each OD pair. Vehicle relocations carried out in Stage-2 are subject to the real-time demand realizations. A virtual relocation zone system is designed, for which, vehicles are bounded in relocation operations. A virtual access zone is further established where clients can walk or bike for a short distance to pick up an available vehicle. In this way, the imbalance problem can be handled by a combination method of trip pricing, vehicle relocation via hiring drivers, and access trips via walking or biking. Three dedicated solution algorithms are developed to solve the combined problem: a gradient search algorithm, a genetic algorithm and an iterated local search algorithm. All algorithms are compared as a means to solve the MINLP for a large case-study area.

The remainder of this paper is organized as follows. In Section 2, the one-way carsharing model under demand uncertainty is introduced. The solution approaches are proposed in Section 3. Section 4

presents the application to the Suzhou Industrial Park (SIP), China. Conclusions and future work directions are presented in the last section.

2 Model formulation

2.1 Problem setting

We consider the one-way carsharing tactical and operational design problem. The aim is to maximize the total profit from the perspective of the carsharing operator. The study region consists of $|I|$ parking stations with a parking station denoted as $i \in I$. A typical day of operation is divided into $|T|$ time steps (or intervals) with an equal time duration. The tactical decisions, which include vehicle fleet size U and carsharing rental rate P_{ijt} for trips from station i to station j starting at time step $t \in T$, should be determined before the operation takes place. Note here, that the latter is associated with demand uncertainty. The carsharing rental rate P_{ijt} is optimized to adjust the demand for carsharing based on an elastic demand function. The operational decisions include vehicle inventory at each time step $V_{it}(\omega)$, vehicle relocations $N_{ijt}(\omega)$, and served demand $Q_{ijt}(\omega)$ from station i to station j at time step t, which changes with the demand formation ω on a particular day.

2.1.1 Assumptions

To further define the problem, we make the following assumptions:

- There are enough parking spaces for vehicle returns, which include prepaid parking by the carsharing operator, roadside parking, or other public parking spaces.
- The carsharing demand is elastic and stochastic. By construction, when rental prices increase, demand is reduced based on an elasticity model. Moreover, demand varies from day to day so that demand uncertainty is introduced.
- The carsharing demand for a day in one parking station follows a Poisson distribution. The demand distribution in different periods of the day depends on the characteristics of the station such as location, land use, convenience level, etc.

To capture the demand uncertainty, we construct several demand scenarios. Let Ξ be the set of demand scenarios and $\mathbf{E}_{\omega} > 0$ be the probability of scenario $\omega \in \Xi$ with $\sum_{\omega \in \Xi} \mathbf{E}_{\omega} = 1$. For each scenario $\omega \in \Xi$, the actual demand is jointly determined by the price (demand elasticity) and stochastic parameter realizations (demand uncertainty). Based on the negative relationship of price and demand in demand-and-supply curve, the expected demand is calculated by the elastic demand function $q_{ijt} exp(\gamma P_{ijt} + \kappa)$ where q_{ijt} is the demand upper bound, P_{ijt} is the rental price and γ, κ are given non-positive parameters (Huang et al., 2020b; Liu et al., 2013; Xu et al., 2018). According to the elastic demand function, a higher rental price results in lower expected travel demand and vice versa. Together with the Poisson distribution assumption, the actual demand in scenario $\omega \in \Xi$ is constructed as $\left[q_{ijt} exp(\gamma P_{ijt} + \kappa) \right]_{\omega}$, where the term in the brackets is the average demand. For simplicity of notation, the scenario subscript is moved inside and we use the expression $q_{ijt}(\omega) exp(\gamma P_{ijt} + \kappa)$ to denote the demand realization in scenario $\omega \in \Xi$.

In summary, the tactical decision variables (U and P_{ijt}) do not change with demand scenario $\omega \in \Xi$, while the operational decision variables N_{ijt} and Q_{ijt} can be written as $N_{ijt}(\omega)$ and $Q_{ijt}(\omega)$ as these change with demand scenario $\omega \in \Xi$.

2.1.2 Virtual zones

In practice, clients may not be able to pick up a car from a parking station near to his/her origin because there are no vehicles available. To model this situation, we construct a virtual access zone for each trip, which is centered at the origin of the trip. The zone radius is determined by the maximum access distance that people are willing to walk or cycle. A client can use any vehicle in his/her virtual access zone depending on car availability. Fig.1a illustrates the construction of the virtual access zone. A client is located at origin i and is heading to destination j. As vehicles may not always be available at the desired origin station i (assuming in this case that there is a station in the client's origin location), we construct a virtual access zone centered at i with a radius of α. Clients can walk or bike a short distance from i to an available vehicle at any station k within his/her virtual access zone, and then drive to their destination j. We use O_{ikjt} to denote the number of clients that start from station i at time step t and walk or ride a bicycle to the intermediate station k to get a rental car and finally drive to station j in the end. The set of stations in the virtual access zone of station i is denoted by I_i^{Circle}. In the following, I_i^{Circle} define the set of stations (in excess of station i itself) in the virtual access zone. The hollow black triangle in Fig.1a represents the client's desired car rental station and the solid purple triangle represents other available car rental stations nearby. For demand occurring at station i, clients can rent a vehicle not only at station i in the black triangle but also at neighboring stations k in purple triangles. In this way, clients have more options where to pick up cars. If there are enough available vehicles parked at origin i, clients departing from this location are serviced first and the trip chain reduces to O_{iijt} with zero access distance.

In carsharing operations, it may not be economically efficient to relocate vehicles for a long distance. To model the distance constraints in vehicle relocations, we further define a virtual relocation zone as the ring area between the radius of α and β (see Fig.1b), where β is the maximum relocation distance. If there are insufficient vehicles at station i represented by the black triangle, we can only relocate vehicles from stations in blue triangles in the corresponding ring area subject to the maximum relocation distance β. Because clients can walk or bike to the stations in the α area, vehicle relocations in the virtual access zone are not necessary.

We assume that the starting point of a request is always at a station location. As such, we can define virtual access zones and virtual relocation zones based on stations instead of trips - each station has one virtual access zone and relocation zone. At the network level, these virtual zones for different stations overlap with each other (see Fig.1c), which significantly increases the computation difficulty. Though the setting of virtual zones simulates the practical vehicle and user movements, we have to claim that allowing access trips and relocations only within the given radius could cut off feasible solutions and thus may lead to loss of optimality.

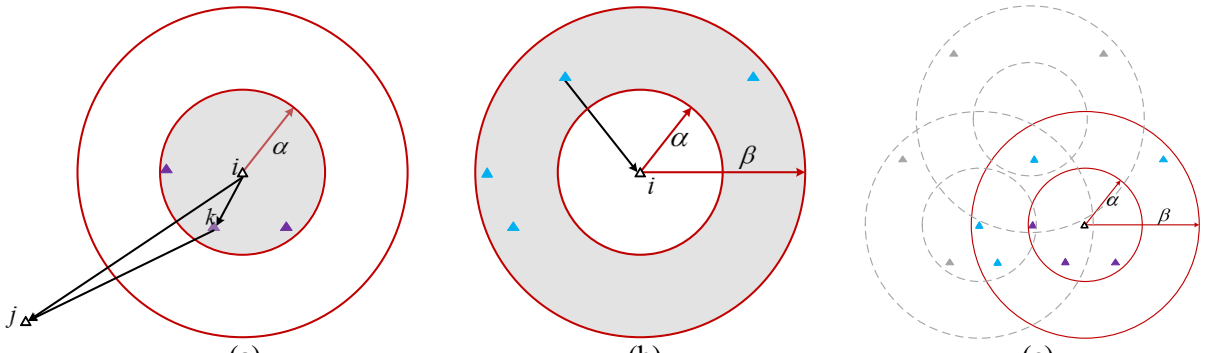

Fig.1 Single/Overlapped virtual zones

Under the explained problem setting, we are ready to formulate the mathematical model for optimizing the price, relocations, and access trips for the one-way carsharing system under demand uncertainty.

2.2 Notation

The notation used throughout the paper is listed below:

Sets	
$I:\{i\},\{k\},\{j\}$	Set of parking stations
I_i^{Circle}	Set of stations in the virtual access zone of station $i \in I$
I_i^{Ring}	Set of stations in the virtual relocation zone of station $i \in I$
$T:\{t\}$	Set of time steps (or intervals)
$\Xi:\{\omega\}$	Set of demand scenarios
Parameters	
c_f	Fixed costs per vehicle per day including depreciation costs and maintenance costs
c_o	Costs of petrol consumption of a vehicle running for one time step
c_r	Fixed Costs of relocating a vehicle per time step
c_a	Access costs of clients by walking or biking per time step
g_{ijt}^{car}	In-vehicle travel time in time steps from parking station $i \in I$ to parking station $j \in I$ departing at the beginning of time step $t \in T$ (time instant $t \in T$)
g_{ikt}^{access}	Access travel time of clients in time steps from parking station $i \in I$ to parking station $k \in I$ departing at the beginning of time step $t \in T$
q_{ijt}	Travel demand upper bound from parking station $i \in I$ to parking station $j \in I$ where $i \neq j$ at time step $t \in T$
α , β	Service radius of virtual zones
M	A positive big number
γ , κ	Non-positive parameters in the elastic demand function
χ , δ	Parameters in the outer-approximation method
$\mathbf{E}_\omega$	Probability of demand scenario $\omega \in \Xi$
Decision variables	
$N_{ijt}(\omega)$	Number of vehicle relocations from parking station $i \in I$ to parking station $j \in I_i^{Ring}$ where $i \neq j$ at the beginning of time step $t \in T$ in scenario $\omega \in \Xi$
$O_{ikjt}(\omega)$	Number of trips departing from parking station $i \in I$ that first walk or bike to intermediate station $k \in I_i^{Circle}$ and then drive to station $j \in I$ where $i \neq j$ at the beginning of time step $t \in T$ in scenario $\omega \in \Xi$
P_{ijt}	Carsharing rental price for trips from parking station $i \in I$ to parking station $j \in I$ where $i \neq j$ at time step $t \in T$
$Q_{ijt}(\omega)$	Number of serviced travel requests from parking station $i \in I$ to parking station $j \in I$ where $i \neq j$ at the beginning of time step $t \in T$ in scenario $\omega \in \Xi$
U	Fleet size of the one-way carsharing system
$V_{it}(\omega)$	Number of vehicles parked in parking station $i \in I$ at the beginning of time step $t \in T$ in scenario $\omega \in \Xi$
Auxiliary variables	
ρ_t	Trip service rate for carsharing at time step $t \in T$
μ_{it} , ν_{it}	Binary variables involved in the linearization of the elastic demand function

2.3 Mathematical model

The stochastic programming model is formulated as follows:

$$\mathbf{P0}\ \max_{P,U,V,N,O,Q}\phi=-c_f U+\mathbf{E}_{\omega\in\Xi}\left[\begin{array}{l}\sum_{t\in T}\sum_{i\in I}\sum_{j\in I}P_{ijt}g_{ijt}^{car}Q_{ijt}(\omega)-\sum_{t\in T}\sum_{i\in I}\sum_{j\in I_i^{Ring}}c_r g_{ijt}^{car}N_{ijt}(\omega)\\ -\sum_{t\in T}\sum_{i\in I}\sum_{k\in I_i^{Circle}}\sum_{j\in I}\left(c_a g_{ikt}^{access}+c_o g_{kjt}^{car}\right)O_{ikjt}(\omega)\end{array}\right] \tag{1}$$

Subject to:

$$U=\sum_{i\in I}V_{i1}(\omega) \qquad \forall\omega\in\Xi \tag{2}$$

$$Q_{ijt}(\omega)\le q_{ijt}(\omega)exp\left(\gamma P_{ijt}+\kappa\right) \qquad \forall i\in I,j\in I,t\in T,\omega\in\Xi \tag{3}$$

$$Q_{ijt}(\omega)=\sum_{k\in I_i^{Circle}}O_{ikjt}(\omega) \qquad \forall i\in I,j\in I,t\in T,\omega\in\Xi \tag{4}$$

$$\sum_{j\in I}Q_{ijt}(\omega)+\sum_{j\in I_i^{Ring}}N_{ijt}(\omega)\le\sum_{j\in I_i^{Circle}}V_{jt}(\omega) \qquad \forall i\in I,t\in T,\omega\in\Xi \tag{5}$$

$$\sum_{k\in I_i^{Circle}}\sum_{j\in I}O_{kijt}(\omega)+\sum_{j\in I_i^{Ring}}N_{ijt}(\omega)\le V_{it}(\omega) \qquad \forall i\in I,t\in T,\omega\in\Xi \tag{6}$$

$$\sum_{k\in I_i^{Circle}\setminus\{i\}}\sum_{j\in I}O_{ikjt}(\omega)=\max\left\{0,\sum_{j\in I}Q_{ijt}(\omega)+\sum_{j\in I_i^{Ring}}N_{ijt}(\omega)-V_{it}(\omega)\right\} \qquad \forall i\in I,t\in T,\omega\in\Xi \tag{7}$$

$$\sum_{k\in I_i^{Circle}\setminus\{i\}}\sum_{j\in I}O_{kijt}(\omega)\le\max\left\{0,V_{it}(\omega)-\sum_{j\in I}Q_{ijt}(\omega)-\sum_{j\in I_i^{Ring}}N_{ijt}(\omega)\right\} \qquad \forall i\in I,t\in T,\omega\in\Xi \tag{8}$$

$$\begin{aligned}V_{it+1}(\omega)=V_{it}(\omega)&-\sum_{k\in I_i^{Circle}}\sum_{j\in I}O_{kijt}(\omega)-\sum_{j\in I_i^{Ring}}N_{ijt}(\omega)+\sum_{j\in I}\sum_{k\in I_j^{Circle}}O_{jkim}(\omega)+\sum_{j\in I_i^{Ring}}N_{jin}(\omega)\\ &\forall i\in I,t\in|T|-1,m=max\left\{0,t+1-\left\lceil g_{jkt}^{access}+g_{kit}^{car}\right\rceil\right\},n=max\left\{0,t+1-\left\lceil g_{jit}^{car}\right\rceil\right\},\omega\in\Xi\end{aligned} \tag{9}$$

$$N_{ijt}(\omega),O_{ikjt}(\omega),Q_{ijt}(\omega),V_{it}(\omega),U\in Z^0,\ P_{ijt}\ge 0 \qquad \forall i\in I,k\in I,j\in I,t\in T,\omega\in\Xi \tag{10}$$

The objective function (1) is to maximize the expected profit for the carsharing operator for a typical day. This is equal to the total revenue minus vehicle fixed costs, relocation costs, access costs, petrol consumption costs. The access cost is the walking or biking distance to pick up vehicles from neighboring stations. Vehicle fixed costs are independent of the demand realization whereas the other costs and revenue all depend on the random demand scenario ω and thus cost expectations $\mathbf{E}_{\omega\in\Xi}[\ ]$ are used.

Constraints (2) represent the fleet size of the carsharing system. The number of allocated vehicles at the beginning of daily operation $\sum_{i\in I}V_{i1}(\omega)$ for each scenario should be the same and is equal to U.

In Constraints (3), $Q_{ijt}(\omega)$ is the serviced carsharing requests in scenario ω, which should be no larger than the demand for scenario ω as calculated by the right-hand side elastic demand function. The price P_{ijt} does not change with the random demand realization ω. Constraints (4) capture demand conservation. The term $\sum_{k\in I_i^{Circle}}O_{ikjt}(\omega)$ is the total number of trips traveling from origin i to destination j at time step t via any intermediate stations $k\in I_i^{Circle}$.

$\sum_{j\in I}Q_{ijt}(\omega)$ plus the number of relocations $\sum_{j\in I_i^{Ring}}N_{ijt}(\omega)$ leaving station i

$\sum_{j\in I_i^{Circle}}V_{jt}(\omega)$ of station i. It states that the serviced requests at station i t

i and its neighboring stations

$\sum_{k\in I_i^{Circle}}\sum_{j\in I} O_{kijt}(\omega)$ and relocated vehicles $\sum_{j\in I_i^{Ring}} N_{ijt}(\omega)$ leaving station i is not larger than the available vehicles in station i.

Constraints (7) state that the clients at origin station i have to take a detour to pick up vehicles in neighboring stations only if there are not enough vehicles available at station i. The term $\sum_{i\in I_i^{Circle}\setminus\{i\}}\sum_{j\in I} O_{ikjt}(\omega)$ in Constraints (7) is the total number of clients that start at origin i at time t and use vehicles in other parking stations $k\neq i$ to get to their destinations, where $k\in I_i^{Circle}\setminus\{i\}$ must be in the access zone of station i. It can also be interpreted as the number of vehicles rented by clients in station i from other stations $k\neq i$. The right-hand side of Constraints (7) calculates vehicle shortage at station i, which is the number of client requests $\sum_{j\in I} Q_{ijt}(\omega)$ plus vehicle relocations $\sum_{j\in I_i^{Ring}} N_{ijt}(\omega)$ minus current vehicle inventory. If there is a vehicle shortage at station i, that is $\sum_{j\in I} Q_{ijt}(\omega)+\sum_{j\in I_i^{Ring}} N_{ijt}(\omega)-V_{it}(\omega)>0$, Constraints (7) ensure this shortage can be covered by diverting clients to neighboring stations. On the other hand, when the inventory at station i can cover all vehicle demand, i.e. $\sum_{j\in I} Q_{ijt}(\omega)+\sum_{j\in I_i^{Ring}} N_{ijt}(\omega)-V_{it}(\omega)\le 0$, such diversion is not allowed. As such, vehicles serve the demand at their station first. Constraints (8) ensure that vehicles at station i can be rented to clients from neighboring stations $k\in I_i^{Circle}\setminus\{i\}$ only if there is vehicle excess supply at this station after fulfilling its own requests. On the left-hand side of Constraints (8), term $\sum_{k\in I_i^{Circle}\setminus\{i\}}\sum_{j\in I} O_{kijt}(\omega)$ is the total number of vehicles parked in station i at time step t rented by clients from neighboring stations $k\neq i$. The right-hand side of Constraints (8) calculates the number of excess vehicle supply in station i at time instant t after fulfilling the clients' requests and relocations. Similar to Constraints (7), the right-hand side of (8) is positive if there is vehicle oversupply and is zero otherwise.

Constraints (9) calculate the number of available vehicles in the next time instant $t+1$. It is equal to the available vehicles V_{it} minus the vehicles leaving to service requests in the access zone $\sum_{k\in I_i^{Circle}}\sum_{j\in I} O_{kijt}(\omega)$ and relocations $\sum_{j\in I_i^{Ring}} N_{ijt}(\omega)$, plus the vehicles $\sum_{j\in I}\sum_{k\in I_j^{Circle}} O_{jkim}(\omega)+\sum_{j\in I_i^{Ring}} N_{jin}(\omega)$ arriving at station at time step t. m is the departure time of clients that will arrive at station i between time instants t and $t+1$. n is the departure time of the relocated vehicles that will arrive at station i between time instants t and $t+1$. The departure time m and n are uniquely determined by the departure station j for a given arrival station i and arrival time $t+1$. Thus, the term m should be m_{jkit}, and the term n should be n_{jit}.

Constraints (10) specify the domain of the decision variables.

Problem **P0** is nonlinear due to the elastic demand function in the objective function and Constraints (3), (7) and (8). We will first linearize these constraints as elaborated in the next sections.

2.3.1 Linearization of the constraints caused by overlapped virtual zones

The non-linear Constraints (7) and (8) caused by overlapped virtual zones incur a great computation challenge, a series of linearization methods are proposed as follows. Since it is a general linearization technique, we omit (ω) in all the decision variables for notation simplicity.

Constraints (7) are replaced by Constraints (11)-(16).

$$\sum_{k\in I_i^{Circle}\setminus\{i\}}\sum_{j\in I} O_{ikjt} \geq 0 \qquad \forall i\in I, t\in T \qquad (11)$$

$$\sum_{k\in I_i^{Circle}\setminus\{i\}}\sum_{j\in I} O_{ikjt} \geq \sum_{j\in I} Q_{ijt} + \sum_{j\in I_i^{Ring}} N_{ijt} - V_{it} \qquad \forall i\in I, t\in T \qquad (12)$$

$$\sum_{k\in I_i^{Circle}\setminus\{i\}}\sum_{j\in I} O_{ikjt} - M\left(1-\mu_{it}\right) \leq 0 \qquad \forall i\in I, t\in T \qquad (13)$$

$$\sum_{k\in I_i^{Circle}\setminus\{i\}}\sum_{j\in I} O_{ikjt} - M\left(1-\nu_{it}\right) \leq \sum_{j\in I} Q_{ijt} + \sum_{j\in I_i^{Ring}} N_{ijt} - V_{it} \qquad \forall i\in I, t\in T \qquad (14)$$

$$\mu_{it} + \nu_{it} \geq 1 \qquad \forall i\in I, t\in T \qquad (15)$$

$$\mu_{it}, \nu_{it} \in \{0,1\} \qquad \forall i\in I, t\in T \qquad (16)$$

When μ_{it}=1 and ν_{it}=0, Constraints (13) reduce to $\sum_{k\in I_i^{Circle}\setminus\{i\}}\sum_{j\in I} O_{ikjt} \leq 0$ and Constraints (14) are redundant. Together with Constraints (11), we have $\sum_{k\in I_i^{Circle}\setminus\{i\}}\sum_{j\in I} O_{ikjt} = 0$ and Constraints (12) reduce to $\sum_{j\in I} Q_{ijt} + \sum_{j\in I_i^{Ring}} N_{ijt} - V_{it} \leq 0$. This indicates that vehicle inventory at station *i* can fulfill all requests and relocations. Hence, user detours from station *i* to *k* are not needed, i.e. $O_{ikjt} = 0$. When μ_{it}=0 and ν_{it}=1, Constraints (14) reduce to $\sum_{k\in I_i^{Circle}\setminus\{i\}}\sum_{j\in I} O_{ikjt} \leq \sum_{j\in I} Q_{ijt} + \sum_{j\in I_i^{Ring}} N_{ijt} - V_{it}$ and Constraints (13) are redundant. Together with Constraints (12) and (11), we have $\sum_{k\in I_i^{Circle}\setminus\{i\}}\sum_{j\in I} O_{ikjt} = \sum_{j\in I} Q_{ijt} + \sum_{j\in I_i^{Ring}} N_{ijt} - V_{it}$ and $\sum_{j\in I} Q_{ijt} + \sum_{j\in I_i^{Ring}} N_{ijt} - V_{it} \geq 0$. It represents that there is a vehicle shortage at station *i* and users have to walk or bike from station *i* to intermediate station *k* and then drive to destination station *j*, i.e. $O_{ikjt} \geq 0$. When μ_{it}=1 and ν_{it}=1, we have $O_{ikjt} = 0$ and $\sum_{j\in I} Q_{ijt} + \sum_{j\in I_i^{Ring}} N_{ijt} - V_{it}$=0. This indicates that vehicles parked in station *i* can just service all the clients' requests and vehicle relocations.

For Constraints (8), we introduce a new auxiliary variable O_{it}^{max} which represents the maximum value of $\sum_{k\in I_i^{Circle}\setminus\{i\}}\sum_{j\in I} O_{kijt}$. We have $O_{it}^{max} = \max\left\{0, V_{it} - \sum_{j\in I} Q_{ijt} - \sum_{j\in I_i^{Ring}} N_{ijt}\right\}$. Via the same linearization technique, Constraints (8) can be substituted by Constraints (17)-(21).

$$\sum_{k\in I_i^{Circle}\setminus\{i\}}\sum_{j\in I} O_{kijt} \leq O_{it}^{max} \qquad \forall i\in I, t\in T \qquad (17)$$

$$O_{it}^{max} \geq 0 \qquad \forall i\in I, t\in T \qquad (18)$$

$$O_{it}^{max} \geq V_{it} - \sum_{j\in I} Q_{ijt} - \sum_{j\in I_i^{Ring}} N_{ijt} \qquad \forall i\in I, t\in T \qquad (19)$$

$$O_{it}^{max} - M\left(1-\nu_{it}\right) \leq 0 \qquad \forall i\in I, t\in T \qquad (20)$$

$$O_{it}^{max} - M\left(1-\mu_{it}\right) \leq V_{it} - \sum_{j\in I} Q_{ijt} - \sum_{j\in I_i^{Ring}} N_{ijt} \qquad \forall i\in I, t\in T \qquad (21)$$

2.3.2 Linearization of the elastic demand function

Another major computation difficulty arises from the elastic demand function in the form of non-linear term $P_{ijt}Q_{ijt}(\omega)$ in the objective function and the non-linear constraints (3). A ε-optimal algorithm is proposed to address such a problem in the following. Again, (ω) in all the decision variables are omitted for simplicity of notation.

Let $F(P_{ijt}) = q_{ijt} exp(\gamma P_{ijt} + \kappa)$, Constraints (3) are rewritten as:

$$Q_{ijt}(\omega) \le F\left(P_{ijt}\right) \qquad \forall i \in I, j \in I, t \in T \qquad (22)$$

Since the carsharing demand decreases with the increase in price, a negative relationship exists between the two. Hence, Constraints (3) can be further reformulated by expressing P_{ijt} as a function of Q_{ijt}:

$$P_{ijt} \le F^{-1}\left(Q_{ijt}\right) = \left(lnQ_{ijt} - lnq_{ijt} - \kappa\right)/\gamma \qquad \forall i \in I, j \in I, t \in T \qquad (23)$$

We replace $P_{ijt}Q_{ijt}$ by $G\left(Q_{ijt}\right)$ in the objective function:

$$G\left(Q_{ijt}\right) = P_{ijt}Q_{ijt} \le F^{-1}\left(Q_{ijt}\right)Q_{ijt} = \left[\left(lnQ_{ijt} - lnq_{ijt} - \kappa\right)/\gamma\right]Q_{ijt} \qquad \forall i \in I, j \in I, t \in T \qquad (24)$$

A new MINLP model is established via substituting $G\left(Q_{ijt}\right)$ by $\left[\left(lnQ_{ijt} - lnq_{ijt} - \kappa\right)/\gamma\right]Q_{ijt}$ in the objective function **P0**. The two models are equivalent and have the same optimal solution, which has been proved by Xu et al. (2018). We use a ε-optimal algorithm in which a piecewise-linear function is built to approximate the non-linear function $G\left(Q_{ijt}\right)$ (Wang and Meng, 2012; Huang et al., 2020b). As shown in Fig.2. ε define the maximum error tolerance implied by the approximation.

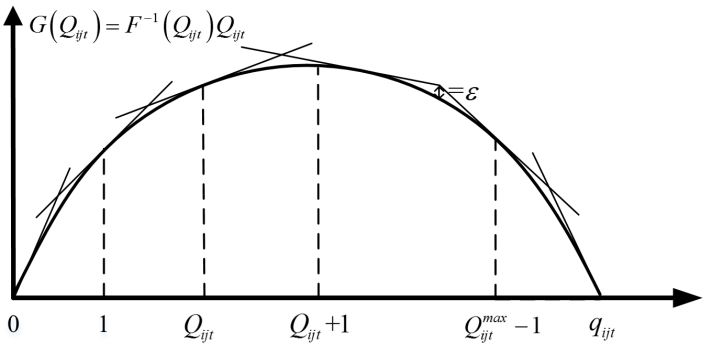

Fig.2 Outer-approximation procedure

The non-linear term $P_{ijt}Q_{ijt}$ in the objective function is thus replaced by a set of linear constraints as shown below.

$$G\left(Q_{ijt}\right) \le \chi^{l}{Q_{ijt}}^{l} + \delta^{l} \qquad \forall i \in I, j \in I, t \in T, l = 1,2,...,L_{ijt} \qquad (25)$$

Constraints (25) impose that the term $P_{ijt}Q_{ijt}$ should be no greater than the given $\left|L_{ijt}\right|$ linear equations $\chi^{l}Q_{ijt}^{k} + \delta^{l} \quad \forall l \in L_{ijt}$, where χ and δ are the slope and intercept respectively.

The original **P0** is thus transformed into a mixed integer linear program (MILP). While it remains an NP-hard problem, small-scale instances with a limited number of demand scenarios can be solved by commercial solvers, such as CPLEX and Gurobi. The number of original constraints (2), (4)-(6), (9)-(10) and the added linearization constraints (11)-(21), (25) all increase with the number of demand scenarios considered. It is well known that the computation time of MILP increases exponentially with the number of constraints. When considering that the number of variables and constraints in the model is already large, solving this MILP by existing solvers is a challenge and is only possible for smaller size problems.

In a test network consisting of 52 stations and 26 time steps, it takes 305 seconds to solve **P0** under one demand scenario by Gurobi. The computation time increases to 2.5 hours when considering three demand scenarios. Four and more scenarios cause memory overflow. To deal with the computation

$N_{ijt}(\omega)$ and client trips $Q_{ijt}(\omega)$ and $O_{ikjt}(\omega)$ are optimized under uncertain travel demand in scenario $\omega \in \Xi$, while the carsharing price P_{ijt} and fleet size U should be optimized by anticipating the expected costs owing to random demand realization.

3 Two-stage stochastic programming model

3.1 Model formulation

According to Constraints (2) and (3), the fleet size U and price P_{ijt} must be the same in all scenarios. This implies that the different scenarios are interdependent and this in turn makes it challenging to solve the large-scale MILP problem. As a consequence, we introduce a novel notion of service reliability to decouple the different scenarios and propose a two-stage stochastic programming model. The long-term tactical decisions and real-time operational decisions are separated in this two-stage optimization. We denote ρ_t as the service rate which is the percentage of carsharing trips that is served at time step t with the set denoted as $\boldsymbol{\rho}=\{\rho_t\}$. Given a service rate $\boldsymbol{\rho}$, Stage-1 aims to determine the price and fleet size such that the average service rate at time step t reaches ρ_t. With the given price and fleet size, Stage-2 is to optimize vehicle relocations under each demand scenario. We then examine $\boldsymbol{\rho}$ to find a promising search direction for which the profit is expected to be maximized. Fig.3 shows the flow chart of the two-stage stochastic programming formulation.

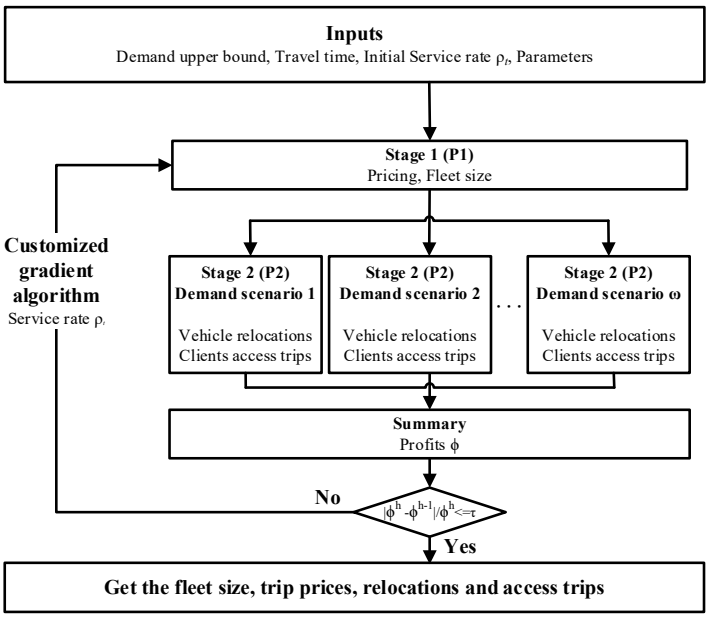

Fig.3 Flow chart of the two-stage stochastic programming formulation

3.1.1 Stage-1

For a given service rate $\boldsymbol{\rho}=\{\rho_t\}$, Stage-1 determines the tactical decisions of price P_{ijt} and fleet size U. Since Stage-1 only considers the expected demand, all the randomness $\omega \in \Xi$ is removed. We introduce $\overline{Q}_{ijt}$, $\overline{O}_{ikjt}$ and $\overline{N}_{ijt}$ as variables that represent client trips and vehicle relocations in Stage-1. The mathematical model of Stage-1 can be written as follows.

$$\begin{aligned} \textbf{P1} \quad \max_{P,U,V,N,O,Q} \phi_2 = & -c_f U + \sum_{t\in T}\sum_{i\in I}\sum_{j\in I} G\left(\overline{Q}_{ijt}\right) g_{ijt}^{car} - \sum_{t\in T}\sum_{i\in I}\sum_{j\in I_i^{Ring}} c_r g_{ijt}^{car} \overline{N}_{ijt} \\ & - \sum_{t\in T}\sum_{i\in I}\sum_{k\in I_i^{Circle}}\sum_{j\in I}\left(c_a g_{ikt}^{access} + c_o g_{kjt}^{car}\right)\overline{O}_{ikjt} \end{aligned} \tag{26}$$

Subject to:

Constraints (2), (4)-(6), (9)-(10), (11)-(21), (25), plus:

$$\frac{\sum_{i\in I}\sum_{j\in I}\overline{Q}_{ijt}}{\sum_{i\in I}\sum_{j\in I}\overline{q}_{ijt}}=\rho_t \qquad \forall t\in T \tag{27}$$

Constraints (27) require that the service rate should be equal to ρ_t. The random variables $Q_{ijt}(\omega)$, $O_{ikjt}(\omega)$, $N_{ijt}(\omega)$ in all the constraints in **P0** should be replaced by the deterministic ones $\overline{Q}_{ijt}$, $\overline{O}_{ikjt}$ and $\overline{N}_{ijt}$ respectively. **P1** thus has a much smaller size which is independent of the demand scenarios and can be readily solved by CPLEX or Gurobi. After solving **P1**, we can obtain the price $\overline{P}_{ijt}$ and fleet size $\overline{U}$, which will be used as inputs to the following Stage-2 problem.

3.1.2 Stage-2

For a given price $\overline{P}_{ijt}$ and fleet size $\overline{U}$, Stage-2 calculates vehicle relocations $N_{ijt}(\omega)$ and client trips $Q_{ijt}(\omega)$ and $O_{ikjt}(\omega)$ for each scenario $\omega\in\Xi$. We rewrite the mathematical model in the following.

$$\begin{aligned}\textbf{P2-}(\omega)\quad \max_{V,N,O,Q}\phi_3(\omega)=&-c_f\overline{U}+\sum_{t\in T}\sum_{i\in I}\sum_{j\in I}\overline{P}_{ijt}Q_{ijt}(\omega)g_{ijt}^{car}-\sum_{t\in T}\sum_{i\in I}\sum_{j\in I_i^{Ring}}c_rN_{ijt}(\omega)g_{ijt}^{car}\\&-\sum_{t\in T}\sum_{i\in I}\sum_{k\in I_i^{Circle}}\sum_{j\in I_i^{Out}}\left(c_ag_{ikt}^{access}+c_og_{kjt}^{car}\right)O_{ikjt}(\omega)\end{aligned} \tag{28}$$

Subject to:

Constraints (4)-(6), (9), (11)-(21), plus:

$$\sum_{i\in I}V_{i1}(\omega)=\overline{U} \tag{29}$$

$$Q_{ijt}(\omega)\le q_{ijt}(\omega)exp\left(\gamma\overline{P}_{ijt}+\kappa\right) \qquad \forall i\in I,j\in I,t\in T \tag{30}$$

$$N_{ijt}(\omega),O_{ikjt}(\omega),Q_{ijt}(\omega)\in Z^0 \qquad \forall i\in I,k\in I,j\in I,t\in T \tag{31}$$

Since the tactical decisions and operational decisions have been decoupled by the service rate **ρ**, the demand scenarios can be handled separately which significantly reduces the computation difficulty. **P2-**(ω) is solved for each demand scenario ω generated, and is repeated $|\Xi|$ times. After solving **P1** and **P2-**(ω), we combine the two stages. The final profit of the system can be calculated as:

$$\phi=-c_f\overline{U}+\sum_{\omega\in\Xi}\mathbf{E}_{\omega\in\Xi}\left\{\begin{array}{l}\sum_{t\in T}\sum_{i\in I}\sum_{j\in I}\overline{P}_{ijt}Q_{ijt}(\omega)g_{ijt}^{car}-\sum_{t\in T}\sum_{i\in I}\sum_{j\in I_i^{Ring}}c_rN_{ijt}(\omega)g_{ijt}^{car}\\-\sum_{t\in T}\sum_{i\in I}\sum_{k\in I_i^{Circle}}\sum_{j\in I}\left(c_ag_{ikt}^{access}+c_og_{kjt}^{car}\right)O_{ikjt}(\omega)\end{array}\right\}, \tag{32}$$

where the carsharing price $\overline{P}_{ijt}$ and fleet size $\overline{U}$ are obtained in **P1**, while other decision variables including serviced demand $Q_{ijt}(\omega)$ and $O_{ikjt}(\omega)$, and vehicle relocations $N_{ijt}(\omega)$ are obtained in **P2-**(ω) under demand realizations $\omega\in\Xi$.

The final profits are calculated based on Eq.(32). Once changing the service rate, the total profits will be changed. The method rationale is to develop a service rate-based solution procedure to solve **P1** and then **P2-**(ω) repeatedly until the stopping criterion is satisfied.

3.2 Optimization algorithm

3.2.1 Gradient search algorithm

We develop a Gradient Search Algorithm (GSA) to solve the two-stage stochastic programming model. With a given service rate $\boldsymbol{\rho}=\{\rho_t\}$ in Constraints (27), we can get the fleet size and price in **P1**, and then optimize the vehicle relocation and access trips in **P2**. The final system profits are obtained in Eq. (32). Via rolling the service rate, we can get a better solution step by step. The update of the gradient is decided by the decent direction vector $\nabla\phi^h$ and step size π_h. The service reliability $\boldsymbol{\rho}^h=\left[\rho_1^h \quad \rho_2^h \quad ... \quad \rho_{|T|}^h \right]$ is a vector. We increase its element once in each time and examine its influence on the objective value (the profit). For example, the initial reliability in iteration h is $\boldsymbol{\rho}^h=\left[\rho_1^h \quad \rho_2^h \quad ... \quad \rho_{|T|}^h \right]$. We increase its element ρ_t^h by δ_t^h while maintaining the other elements in the vector unchanged, i.e. set $\boldsymbol{\rho}_t^h=\left[\rho_1^h, \rho_2^h \quad ... \quad \rho_t^h+\delta_t^h \quad ... \quad \rho_{|T|-1}^h, \rho_{|T|}^h\right]$ and calculate the objective value ϕ_t^h. By comparing the profit difference, we can obtain the ratio of changes $\left(\phi_t^h-\phi^h\right)/\delta_t^h$. After doing the same for all elements in $\boldsymbol{\rho}_t^h$, we can obtain the decent direction in the form of vector which is written as $\nabla\phi^h$. Step size of π_h is calculated in the equation $\pi_h=\lambda_h\left(\phi^h-\gamma_1\phi^*\right)/\left\|\nabla\phi^h\right\|^2$. The utilization of a service rate vector (time dependent service rates) allows different reliabilities for different time periods. Otherwise, a fixed value of service rate may lead to sub-optimality. Moreover, higher service rates happen at off-peak hours, but lower service rates occur at morning and afternoon peak hours. Time dependent service rate also better captures the reality. Please note that we cannot ensure that a global optimum is obtained. This algorithm tries to find a better solution step by step until a local optimum is reached. The following pseudo-code shows such an algorithm. Let h be the iteration number and ϕ be the objective function value.

Step 1: Set $h=1$, initialize $\boldsymbol{\rho}=\boldsymbol{\rho}^h$.

Step 2: Given $\boldsymbol{\rho}^h$, optimize model **P1** to get the carsharing price $\overline{P}_{ijt}$ and fleet size $\overline{U}$, and then use the given price and fleet size to optimize model **P2** and get the vehicle relocations, and then calculate the profit by Eq.(32). The final profit $\phi^h\left(\boldsymbol{\rho}^h\right)$ can be obtained.

Step 3: Update the maximum objective value, and save it as ϕ^*.

Step 4: If $\left|\phi^h-\phi^{h-1}\right|/\phi^h\le\tau$, stop. Otherwise, proceed to Step 5.

Step 5: Determine the optimal $\boldsymbol{\rho}$.

Step 5.1: Calculate the partial derivative of ϕ^h with respect to ρ_t as below.

Step 5.1.1: Given $\boldsymbol{\rho}^h$ as the following $|T|$ dimensional vector and its corresponding objective value ϕ^h, $\boldsymbol{\rho}^h=\left[\rho_1^h \quad \rho_2^h \quad ... \quad \rho_{|T|}^h \right]$, do the following for each element in $\boldsymbol{\rho}^h$.

Step 5.1.2:

a. Set $\boldsymbol{\rho}_t^h=\left[\rho_1^h, \rho_2^h \quad ... \quad \rho_t^h+\delta_t^h \quad ... \quad \rho_{|T|-1}^h, \rho_{|T|}^h\right]$, where δ_t^h is a small positive number.

b. If $\rho_t^h+\delta_t^h>1$, go to Step e. Otherwise, proceed to Step c.

c. Solve **P1** and **P2** with given $\boldsymbol{\rho}_t^h$. If $\phi_t^h\ne\phi^h$, go to Step 5.1.3; otherwise set $\delta_t^h=\delta_t^h+\delta^0$, where the small positive number δ^0 is the step size.

d. Go back to Step a.

e. Set $\boldsymbol{\rho}_t^h=\left[\rho_1^h, \rho_2^h \quad ... \quad \rho_t^h-\delta_t^h \quad ... \quad \rho_{|T|-1}^h, \rho_{|T|}^h\right]$; solve **P1** and **P2** with given $\boldsymbol{\rho}_t^h$. If

---

$\phi_t^h \neq \phi^h$, go to Step 5.1.3; otherwise set $\delta_t^h = \delta_t^h + \delta^0$.

f. If $\rho_t^h - \delta_t^h > 0$, go to Step e. Otherwise, the sensitivity of ρ_t^h is set to zero.

Step 5.1.3: The sensitivity of element ρ_t^h can be obtained: $\Delta\phi^h / \Delta\rho_t^h = \left(\phi_t^h - \phi^h\right) / \left(\rho_t^{h'} - \rho_t^h\right)$, where $\rho_t^{h'} = \rho_t^h + \delta_t^h$ or $\rho_t^{h'} = \rho_t^h - \delta_t^h$.

Step 5.1.4: If $t \neq |T|$, set $t = t+1$, and go to Step 5.1.2. Otherwise, the whole set of sensitivities of ϕ^h with respect to $\boldsymbol{\rho}^h$ has been obtained, denoted by the vector $\nabla\phi^h$.

Step 5.2: Take the sensitivity vector $\nabla\phi^h$ as the descent direction. The step size π_h is chosen in the same way as in Wang and Lo (2008): $\pi_h = \lambda_h \left(\phi^h - \gamma_1 \phi^*\right) / \left\|\nabla\phi^h\right\|^2$. $\gamma_1\phi^*$ is an estimate of the minimum of ϕ^h. The value of parameters γ_1, λ_h should be specified for different model applications.

Step 5.3: Calculate the service rate $\boldsymbol{\rho}^{h+1} = \boldsymbol{\rho}^h + \pi_h \nabla\phi^h$. Project the new value $\boldsymbol{\rho}^{h+1}$ onto the feasible space $[0,1]$; this result is set to be the service rate $\boldsymbol{\rho}^{h+1}$ for the next step. Set $h = h+1$, and go to Step 2.

To save computation time, parallel computing is adopted in Step 2 in the GSA. In Stage-2, **P2** models for different demand scenarios $\omega \in \Xi$ are independent and thus can be solved at the same time with multiprocessing modules in parallel computing. In this way, the computation time of the Stage-2 problem is reduced to $1/\Xi$.

3.2.2 Genetic algorithm

To demonstrate the efficiency of the GSA, we also develop a genetic algorithm (GA) to solve the two-stage stochastic programming model. One chromosome can be decoded for a $\boldsymbol{\rho}$. The solution update is facilitated by swapping genes in the chromosome. The following shows the pseudo-code. Let h be the iteration number, ϕ be the objective function value, ψ be the population size, η be the chromosome length, o be the crossover rate, π be the mutation rate.

Step 1: Set $h = 1$, randomly generate initial population size ψ^h with the chromosome length η.

Step 2: Given ψ^h, convert binary chromosome to decimal service rate $\boldsymbol{\rho}^h$.

Step 3: Given $\boldsymbol{\rho}^h$, optimize the model **P1** to get the carsharing price $\overline{P}_{ijt}$ and fleet size $\overline{U}$, and then optimize the model **P2** and get the vehicle relocations, finally calculating the profit using Eq.(32). The final profit $\phi^h\left(\psi^h\right)$ can then be obtained.

Step 4: If h is equal to the maximum iteration number, stop and return the maximum objective value $\phi^h\left(\psi^h\right)$. Otherwise, proceed to Step 5.

Step 5: Create a new population ψ.

Step 5.1: Generate a random value. If the random value is less than the crossover rate o, generate an initial population by combining a father chromosome and mother chromosome; otherwise, go to Step 5.2.

Step 5.2: Generate a random value. If the random value is less than the mutation rate π, update the initial population via random swapping the genes in chromosomes; otherwise, go to Step 5.3.

Step 5.3: Calculate the fitness based on the profit $\phi^h\left(\psi^h\right)$ in Step 3 via a fitness function which is equal to the current profit minus the minimum profit in the population.

Step 5.4: Generate a new population ψ^{h+1} based on the updated initial population and

probability of fitness. Set $h = h + 1$, and go to Step 2.

Similarly, we adopt parallel computing in Step 3 of the GA. Moreover, the computation time can be further reduced to $1/|\psi|$ if individual optimization in a population is solved simultaneously by using parallel computing.

3.2.3 Iterated local search algorithm

An Iterated Local Search Algorithm (ILSA) is also used to further explore the neighborhood of the solutions obtained by the GSA and GA. We set a neighbor threshold of $\boldsymbol{\rho} \in \left[\underline{\boldsymbol{\rho}}, \overline{\boldsymbol{\rho}}\right]$ and a fixed small positive number δ to mimic the perturbation in service rate. There will be $\left(\overline{\rho_t} - \underline{\rho_t}\right)/\delta + 1$ values of ρ_t in each time step and $\left[\left(\overline{\rho_t} - \underline{\rho_t}\right)/\delta + 1\right]^{|T|}$ iterations for the whole search algorithm. For the $\boldsymbol{\rho}$ obtained by the GSA or GA, we firstly optimize model **P1** to get the carsharing price $\overline{P}_{ijt}$ and fleet size $\overline{U}$, and then use them to optimize model **P2**. The profit $\phi(\boldsymbol{\rho})$ can be obtained by Eq.(32). Also, to save computation time, parallel computing in Step 3 is adopted in Iterated local search algorithm.

4 Case study

4.1 Setting up the case study

To demonstrate the applicability of the proposed models and algorithms, the traffic network of SIP in Suzhou, China (traffic zones and travel time information) is used. The area is divided into a total of 54 zones: residential zones from #1 to #20, industrial zones from #21 to #40, commercial zones from #41 to #50 and undeveloped land from #51 to #54. A carsharing station is assumed to be located at the centroid of each zone. We consider 13 hours' of operation time from 7:00 to 20:00, which are divided into 26 time steps with a duration of 30 minutes each. It is further assumed that daily carsharing requests departing from one zone follow a Poisson distribution. A total of Ξ=30 demand scenarios are generated for each zone (see Fig.4 for three example zones). Most existing studies adopt 7 scenarios for a week or 30 scenarios for a month in carsharing case analysis (Brandstätter et al., 2017; Biondi et al., 2016; Fan, 2014; He et al., 2017; 2020). Yet having more scenarios could further improve the robustness of the optimization results. (Lu et al., 2018).

Refer to Fig.4(a) as an example of the daily carsharing requests in zone #5. It follows a Poisson distribution with a mean value of approximately 860. The carsharing requests leaving one zone throughout a typical day are seen in Fig.5 (for average time-varying departures). The random demand generation of Zone 5 at 8:00-8:30 can be considered as an example. It is a residential zone with the demand ratio of 8:00-8:30 over a whole day calculated by 110/935 (see the blue line in Fig. 5). Suppose on a particular day, the realized trip departures from zone #5 for a day is 800. The departures at 8:00-8:30 should be 800*110/935=94.

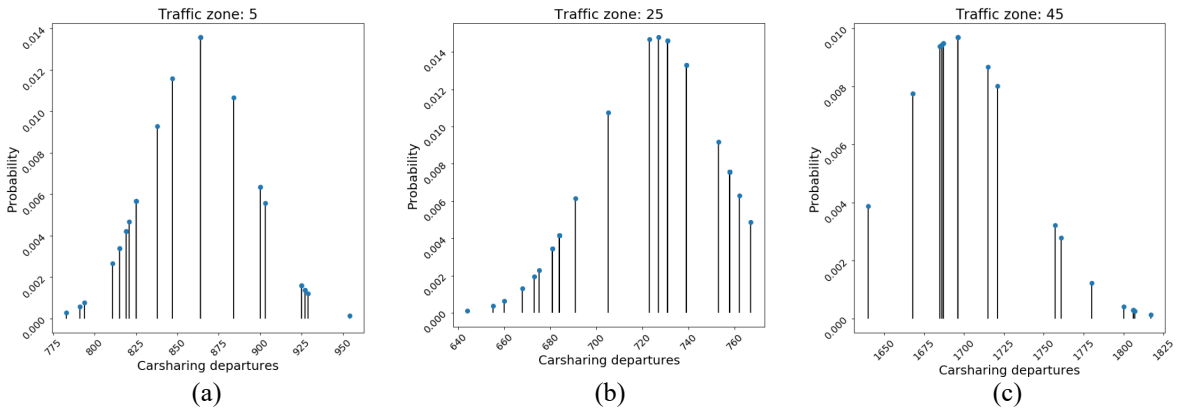

(a) (b) (c)

Fig.4 Poisson distribution of travel requests in one day

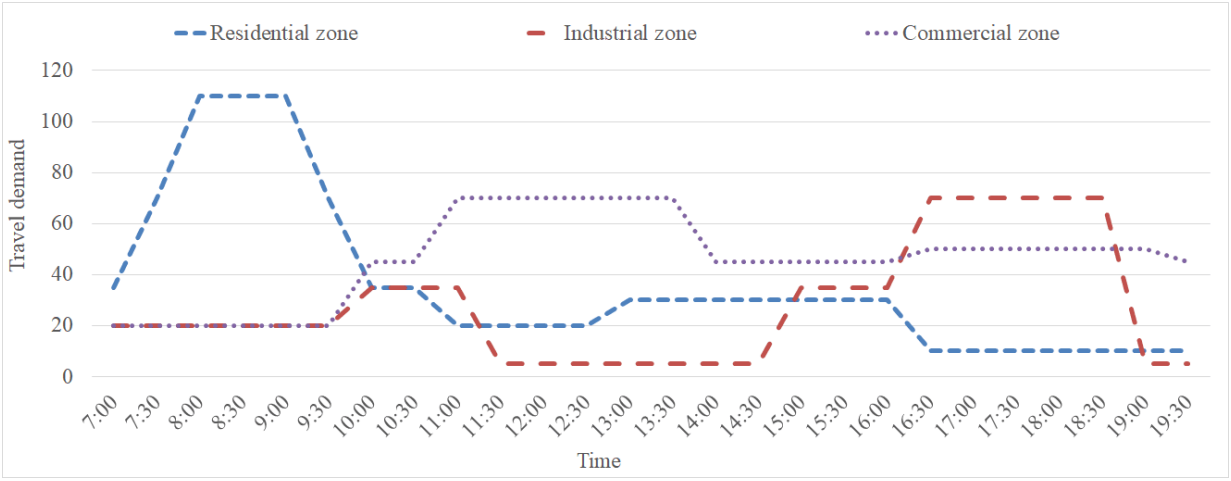

Fig.5 Average time-varying departures

The free flow travel time on the shortest paths is represented as the base travel time, and the average free-flow travel speed of vehicles is set to 25 km/h. The delay time caused by traffic congestion at peak hours is simulated by setting growth factors in different time steps, as shown in Table 2. The in-vehicle travel time g_{ijt}^{car} is equal to the free-flow travel time multiplied by the growth factors. In the case study, we assume clients ride dockless sharing bicycles with an average speed of 10 km/h to pick up vehicles in neighboring zones. The access travel time g_{ijt}^{access} by bike equals 2.5 times the free-flow travel time, and it is not affected by traffic congestion.

Table 2 Growth factors of travel time in relation to the shortest travel time

Time	7:00-7:59; 19:00-19:59; 20:00-6:59[+1]	11:00-11:59; 14:00-15:59	12:00-13:59	10:00-10:59; 18:00-18:59	8:00-9:59; 16:00-17:59
Growth factor	1.0	1.1	1.2	1.3	1.5

In this paper, the parameters to be applied in the model are based on a one-way carsharing company (EVCARD) operating in SIP, China (SIP, 2017; EVCARD, 2021), and previous studies (Huang et al., 2018; Huang et al., 2020a). The vehicle fixed cost c_f is set as ￥100 per veh*day, petrol consumption cost c_o is ￥20 per hour, vehicle relocation cost c_r is ￥80 per hour, and client access cost by riding a bicycle c_a is ￥30 per hour. The radius of the virtual zones α and β are set as 1 km and 4 km respectively. The parameters γ and κ in the elastic demand function are set to -0.0231 and 0. The daily operations are divided into 3 periods: morning peak hours from 7:00 to 10:59, noon peak hours from 11:00-15.59, and afternoon peak hours from 16:00 to 19:59.

4.2 Results

The proposed two-stage stochastic programming model is solved by Python calling Gurobi 7.0.2 solver on an i7 processor @3.60GHz, 48GB RAM computer with a Windows 10 64 bit operating system. Parallel computing is adopted by using 6 processors in solving the Stage-2 problem. In the gradient search algorithm, the Stage-1 model and Stage-2 models are solved sequentially for 23 iterations until the stopping criterion is met. The total computation time is 11.5 hours. The total profits are ￥240,580, average price is ￥78/h, fleet size is 1,010 and average service rate is 85.78%.

4.2.1 Carsharing tactical decisions

Fig.6 shows the price fluctuations over time in the three types of zones. It is found that there is a positive relationship between the carsharing price and the time-varying demand. Higher demand leads to higher prices, and high prices conversely reduce demand for carsharing during peak hours. Take the morning peak hours as an example, the carsharing trips leaving the residential zones experience a significantly higher price than the trips from the other two types of zones. Fig 5 shows the average of

q_{ijt} in the demand elastic function. This can also be interpreted as the total demand for many competing modes including carsharing, taxi and bus. Intuitively, filling all the peak demand in the morning peak by carsharing is inefficient from an economic perspective as it requires a large fleet of vehicles. Many vehicles could be idle during off-peak hours. Hence, a high price is set at peak hours to reduce the carsharing demand to obtain maximum daily profits.

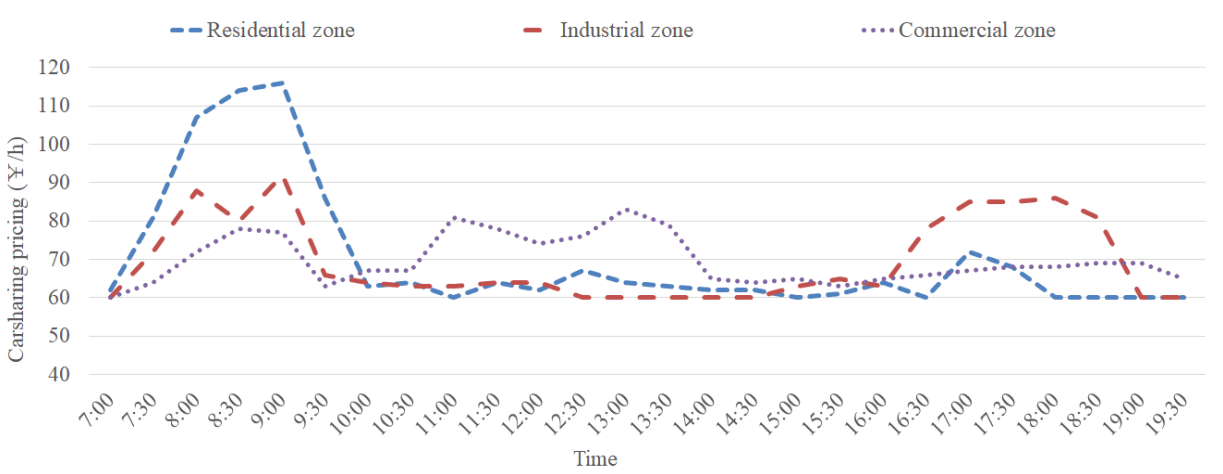

Fig.6 Time-varying price

4.2.2 Carsharing operational decisions

The optimization results for the carsharing operational decisions obtained via the gradient search algorithm are shown in Table 3, where the minimum value, mean value, and maximum value in the 30 demand scenarios are provided. The total profits have minor fluctuations in the 30 scenarios. Their average is ￥240,580 and the Coefficient of Variation (C.V) is 0.85%. Over 84% demand can be satisfied, which equals the number of serviced trips divided by the actual demand for carsharing. A high demand service rate demonstrates the effectiveness of the combination strategy of price incentives and relocations under stochastic demand. As complete service of demand is not required, the operator may reject some non-profitable client requests. As a result, 16% demand is rejected due to the profit maximization objective of the operator. In addition, the demand-supply imbalance also contributes to the demand loss. It can be noted that a total of 405 vehicle relocations are required to tackle the vehicle demand-supply imbalance problem. Moreover, a total of 659 access trips were created where clients took detours to pick up vehicles in the neighboring stations. The relocations and access trips contribute to around 10% of the serviced trips. Another main reason is that the demand in this problem is considered to be stochastic. Vehicle shortage may eventually be amplified if random demand realizations surged in several neighboring zones. It is challenging to use the given fleet size obtained in the tactical decision level to service all demand in the different scenarios. Moreover, Table 3 shows that all C.Vs are no larger than 7.00%.

Table 3 Optimization results in Stage-2

	Profits (￥1,000)	Service rate (%	Relocations	Access trips
Minimum value	234	83.74	362	565
Mean value	241	85.78	405	659
Maximum value	245	87.39	464	712
C.V	0.85%	1.27%	6.85%	6.33%

We randomly select a demand scenario as an example to present more details concerning the operational performance including carsharing demand service rate, the number of vehicle relocations, and access trips. The optimization results for all the 30 scenarios are shown in the Appendix.

The carsharing demand service rate for the 50*50 OD pairs is shown in Fig.7, where the column number represents the origin index and the row number represents the destination index. The grayscale indicates that there is no carsharing demand for this specific OD pair. The green-yellow-red cells

indicate an increasing demand service rate. The number in each cell shows the exact demand service rate %. Fig.7(a) shows the average demand service rate for a whole day between each OD pair. More yellow and red cells indicate a higher service rate. Fig.7(b) is the demand service rate in the morning peak hours. We use the black frame to emphasize the carsharing demand leaving and arriving at residential zones. Most trips in the black frame can be serviced. Especially in the upper-left cells, the red and yellow cells are much denser. It indicates that most demand traveling within the residential zones is serviced due to the high vehicle supply in morning peak hours. The cells in the black frame of Fig.7(c) are trips leaving or arriving at commercial zones at noon peak hours. Overall, the trip service rates are more evenly distributed while the zones in the black frame have relatively more red/yellow cells, or equivalently a higher demand service rate. Fig.7(d) presents carsharing service rates in the afternoon peak period. The black frame emphasizes trips leaving and arriving at industrial zones. A similar trend as in the morning peak is observed.

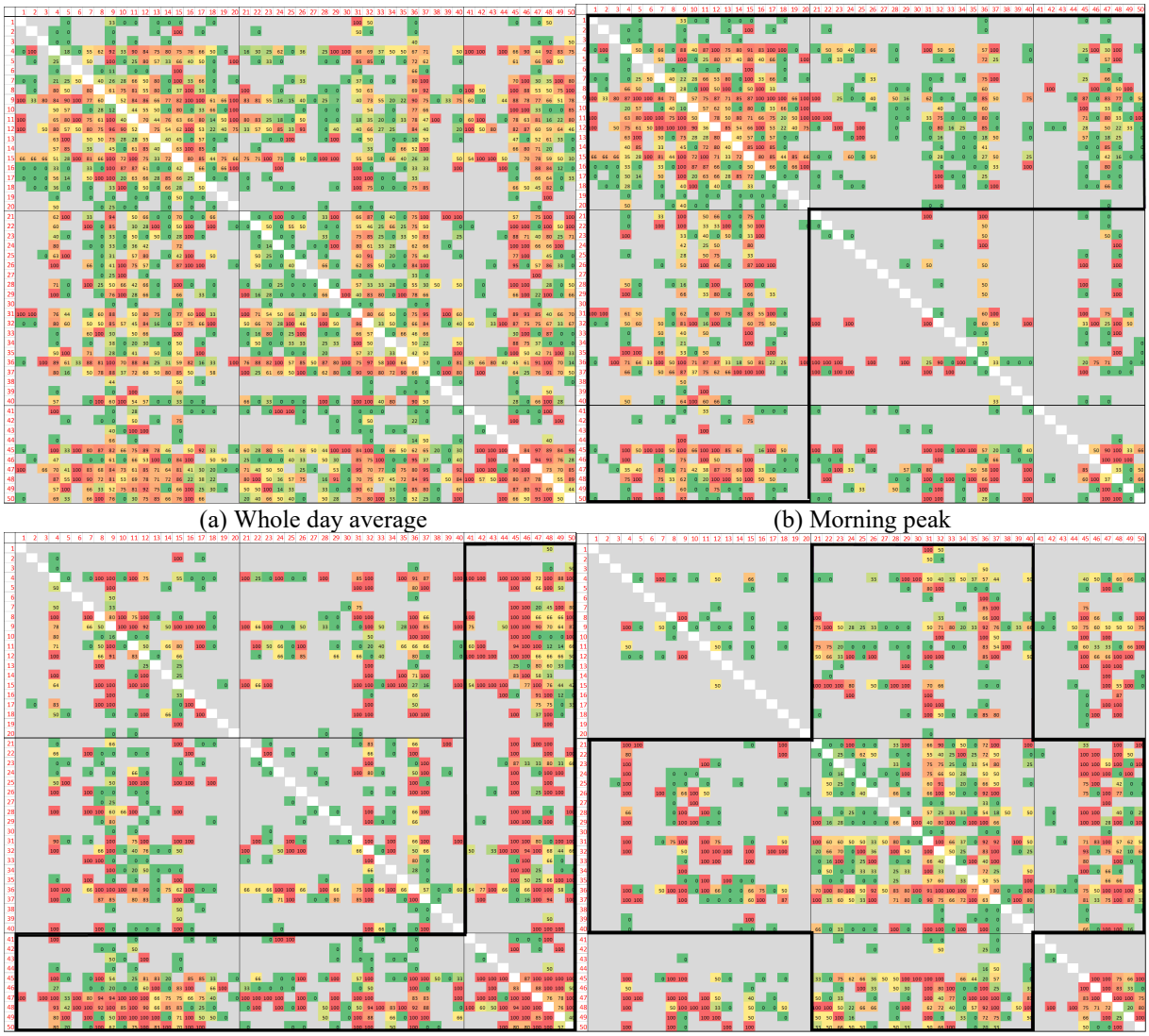

(a) Whole day average (b) Morning peak

(c) Noon peak (d) Afternoon peak

Fig.7 Carsharing demand service rates (%)

There are 440 vehicle relocations in this scenario. Fig.8 shows the vehicle relocation distribution in the SIP area. The green/red scales show the number of vehicles relocated in/out of the zone. A darker color indicates more vehicle relocations. The negative value indicates the number of vehicles relocated into this zone and positive values mean the number of vehicles relocated out of this zone. Grayscale indicates that no vehicle relocations happen in the zone. The vehicle relocations that happen in the morning, noon, and afternoon peak hours are presented in Fig.8(a), (b), and (c), respectively. In Fig.8(a), many vehicles are relocated into residential zones, such as zones #9, #11, and #12. It is because of the

huge carsharing demand occurring in these zones in the morning hours. The commercial zones at noon peak hours and industrial zones at afternoon peak hours indicate a similar pattern in which vehicles are relocated into these zones to address the imbalance problem. Recall that, according to the model, relocations only happen inside the virtual relocation zones. For example, regarding zone #46 in Fig.8(b) as an example, 33 relocations are conducted using vehicles from nearby zones #1, #20, #36 and #39, these are inside the border of the virtual relocation zone of zone #46.

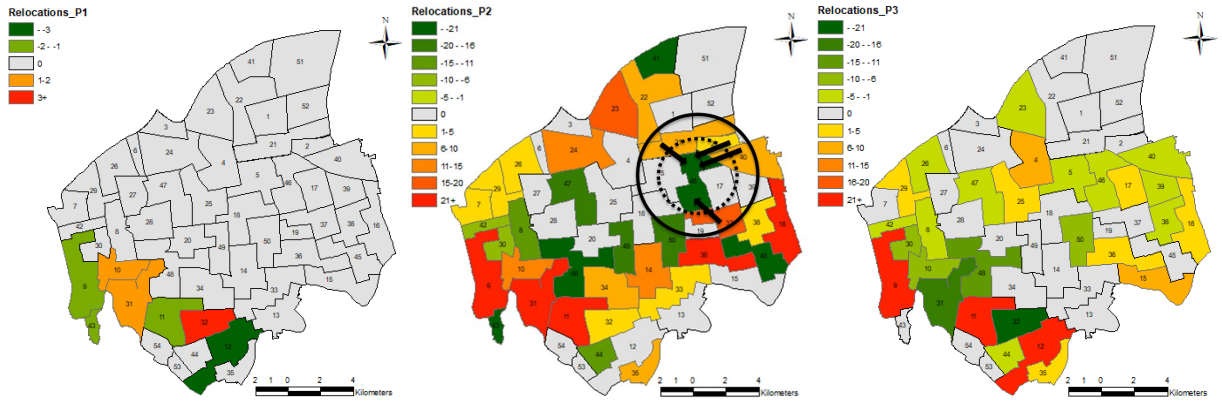

(a) Morning peak (b) Noon peak (c) Afternoon peak

Fig.8 Relocation trip distribution

Fig.9 represents the number of trips in which clients have to bike to another neighboring station to pick up a vehicle because of the vehicle shortage at their desired pick-up location. We use the green/red scales to show the number of access trips in Fig.9. The negative values indicate the number of clients arriving at this zone and the positive values correspond to the number of clients leaving this zone. Fig.9(a) is the access trip distribution in the morning peak. As the carsharing demand is highly concentrated in the morning peak, many clients choose to pick up vehicles from their neighboring zones. As shown in Fig.9(a), the black dotted circle represents the virtual access zone for station #17. Clients can cycle from station #17 to #39 and #46 in the access zone to pick up a vehicle. Fig.9(b) and (c) show the access trip distribution at the noon and afternoon periods. A similar pattern is observed in that many access trips are leaving the commercial zones at noon and the industrial zones at the afternoon peak. In this way, the vehicle imbalance problem can be further mitigated.

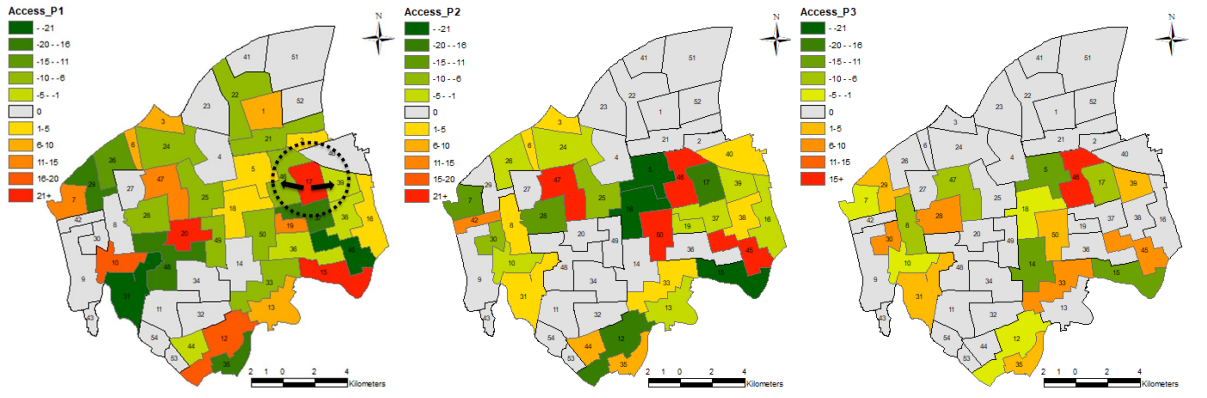

(a) Morning peak (b) Noon peak (c) Afternoon peak

Fig.9 Access trips distribution

Moreover, in comparing Fig.8 to Fig.9, it can be noted that the vehicle relocations and client access trips to a station are complementary. In the morning peak hours, fewer relocation trips occur as can be seen in Fig.8(a) but more access trips happen as seen in Fig.9(a). The main reason is that clients have to bike for vehicle pick-up if vehicles cannot be relocated into their origins in time. In contrast, it is

unnecessary for clients to rent vehicles from neighboring stations if the vehicles' shortage can be handled by relocations.

4.3 Analysis of system performance

4.3.1 Virtual zone size

In this section, we conduct a sensitivity analysis on the size of virtual access zones and virtual relocation zones by setting different service radiuses. Four cases are examined: Case 1 with α=1 km and β=4 km; Case 2 with α=0 and β=4 km; Case 3 with α=1 km and β=0; Case 4 with α=1 km and $\beta=+\infty$. Case 1 is a base case considering both access trips and relocation operations in virtual zones. Case 2 allows relocation operations alone. Case 3 allows access trips alone. Case 4 is an extreme case of Case 1 that the maximum relocation distance can be infinity. Table 4 shows the optimization results.

Table 4 Optimization results of different virtual zone sizes

Case	Stage-1			Stage-2			
	Average price (￥/h)	Fleet size		Profit (￥1,000)	Service rate (%)	Relocations	Access trips
1 α=1, β=4	78	1,010	Minimum value	234	83.74	362	565
			Mean value	241	85.78	405	659
			Maximum value	245	87.39	464	712
2 α=0, β=4	78	1,038	Minimum value	231	88.55	810	0
			Mean value	235	88.96	835	0
			Maximum value	237	89.60	890	0
3 α=1, β=0	79	845	Minimum value	209	74.11	0	563
			Mean value	216	75.81	0	616
			Maximum value	220	76.92	0	685
4 α=1, $\beta=+\infty$	78	983	Minimum value	237	83.41	370	610
			Mean value	241	85.11	399	698
			Maximum value	244	86.12	439	751

The comparison between the proposed access trips & relocations and relocations alone can be found in Case 1 and Case 2. When the access distance reduces from 1 km to 0 km, the average number of access trips naturally reduces to zero while the average number of vehicle relocations increases substantially by 106.17%. When access trips are not allowed in the carsharing system, more vehicle relocation operations are carried out to address the imbalance problem. In this way, more drivers should be employed and larger labor burden occurs. Moreover, the fleet size in Case 2 increases by 2.77% that may lead to traffic burden. The total profit decreases slightly due to the lack of access trips. It indicates that allowing access trips plays an important role in this carsharing system.

The comparison between the proposed access trips & relocations and access trips only can be found in Case 1 and Case 3. It reveals that when we reduce the outer radius of the virtual relocation zone from 4 km to 0 km, no vehicle relocations are performed. The fleet size, profits, and demand service rate drop significantly. Even though the higher price is set to reduce clients' demand and access trips are allowed for vehicle pick-up, the imbalance problem cannot be properly managed. As a result, 24% of the requests cannot be serviced. It supports previous research conclusions that one-way carsharing performance is critically dependent on real-time vehicle relocations.

In Case 4, we expand the outer radius of the virtual relocation zone to infinity. Comparing to Case 1, the same average total profits are obtained, and the difference in fleet size, average demand service rate, average number of relocations, and average access trips between the two cases are 2.67%, 0.78%, 1.48%, and 5.92%, respectively. A similar performance between the two cases demonstrates that setting proper virtual relocation zones can maintain high profits for the carsharing operator whilst not reducing the served demand. Please note that whether relocations are profitable is also dependent on the tradeoff between different cost components.

We made the comparative analysis via setting β=1, β=1.5, β=2, β=2.5, β=3, β=3.5, β=4, and β=+∞. The Profit changes are shown in Fig.10. With the increase of the outer radius β in the virtual relocation zone, the profit increases. It indicates that the proposed virtual relocation zones will cut off some feasible solutions and thus may lead to loss of optimality. However, no larger profit is obtained when enlarging β to positive infinite. It represents that β=4 in this paper is acceptable that might not cut off feasible solutions.

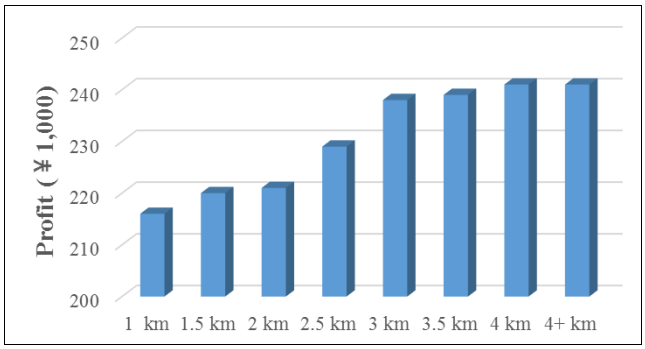

Fig.10 Profit changes under different outer radius β

4.3.2 Cost components

We conduce sensitivity analysis on unit relocation cost (c_r=40, 80, 120 ¥/hour) and unit access trip cost (c_a=20, 30, 40 ¥/hour) respectively. The other parameters are maintained the same as in the base case with c_r=80 and c_r=30. To virtually illustrate the connections between the relocation and access trips, we plot out the percentage of changes in the performance measures of the four added cases comparing to the base case. According to Fig.11(a) and (b), we found that the number of access trips and the number of relocation trips changes inversely, in order to handle the imbalance problem. Yet neither of them has significant impacts on the average price, fleet size and service rate. This further proves the complementary effects of relocation and access trips in dealing with demand supply imbalance problem.

When increasing the unit relocation cost from 40 to 120¥/hour, fewer relocations are carried out yet more access trips occur. As a consequence, the profit and service rate also drop a little. When increasing unit the access cost from 20 to 40 ¥/ hour, fewer clients are rerouted to pick up vehicles in neighboring zones, but more vehicle relocations occur.

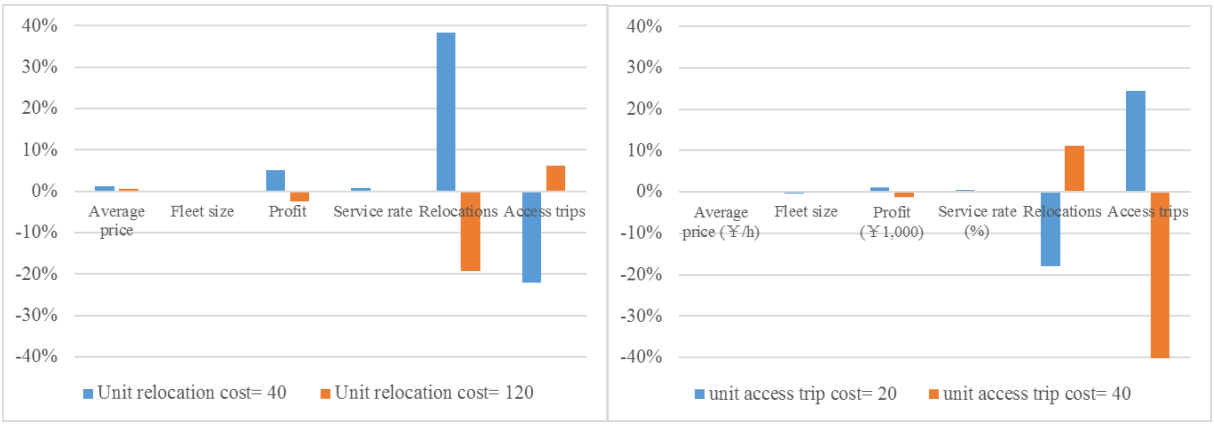

(a) sensitivity on relocation cost (b) sensitivity on access trip cost

Fig.11 Comparative analysis with base case (c_r=80 and c_r=30)

4.3.3 Uncertain demand

The performance of the stochastic programming model is tested by fixing solutions in the out-of-sample scenarios.

Firstly, we carried out an out-of-sample test by generating 100, 200, 500 and 1,000 scenarios assuming the carsharing demand for a day in one parking station follows a Poisson distribution. It takes 2.58 hours, 4.52 hours,8.24 hours, 16.50 hours, respectively. Another group of tests is conducted assuming Normal distribution with C.V of 0.05 and 0.1 with 30 scenarios. As shown in Table 5, The profits obtained in 100, 200, 500 and 1,000 scenarios are slightly lower than that in the base case. The maximum gaps in profits and service rate are 0.69% and 0.33%, respectively. In the case of Normal distribution test, the profits decrease by 20.33%-26.14%. The service rates also drop by 0.09%-6.54%. It indicates that a different distribution pattern has significant impacts on the solution performance. A careful fitting of the demand distribution pattern or careful selection of representative demand scenarios is important.

Table 5 Optimization results with different demand scenario size

		Profits (￥1,000)	Service rate (%)
Poisson distribution (100 Scenarios)	Minimum value	220	81.19
	Mean value	241	86.06
	Maximum value	249	88.67
Poisson distribution (200 Scenarios)	Minimum value	224	81.48
	Mean value	241	86.00
	Maximum value	249	88.75
Poisson distribution (500 Scenarios)	Minimum value	122	58.75
	Mean value	238	85.67
	Maximum value	249	89.08
Poisson distribution (1,000 Scenarios)	Minimum value	147	63.26
	Mean value	240	85.79
	Maximum value	250	88.96
Normal distribution (C.V = 0.05)	Minimum value	174	83.46
	Mean value	198	84.88
	Maximum value	234	86.54
Normal distribution (C.V = 0.1)	Minimum value	121	72.91
	Mean value	184	80.05
	Maximum value	227	85.99

Though demand uncertainty is carefully considered in optimizing the strategic decisions, it is still a challenge to guide vehicle relocation when a demand realization different from estimation occurs. Please note that the relocation plan could change from day to day according to the estimated demand scenario. In the transit timetable design problem (Shakibayifar et al., 2017), when demand overflow occurs, waiting passengers can be regarded as lost (Lee et al., 2014) or flexible dial-a-ride services are provided as dynamic supplements (Chen and An, 2021). Similarly, in the carsharing system, if a different demand scenario other than the estimated one occurs, we could either allow client loss or adjust the relocation plan to maintain a minimum number of vehicles at a station.

4.4 Analysis of solutions

4.4.1 Comparative analysis between integrated and separated approaches

We build a separated model, which solves tactical and operational decisions respectively. Tactical decision model **P1'** is the same as **P1** but with service rate Constraints (27) removed. Operational decision model **P2'** (ω) is exactly the same as **P2** (ω). Constraints (27) are no longer required since the connection between the tactical and operational decisions is intentionally broken. Only price and fleet size are optimized in the tactical level problem **P1'**, and its solutions are used as inputs to the operational level problem **P2'** (ω) under different scenarios. The simplified problem **P1'** is solved once and **P2'** (ω) is solved $|\Xi|$ times. No feedback loop is required. The profit of the system can be calculated by Equation (32).

We conduct 3 groups of comparative analysis on the integrated and separated approaches via using 10, 15 and 30 demand scenarios respectively. Table 7 presents the solution results.

Table 7 Comparative analysis of the solutions obtained by integrated and separated approaches

No. of scenarios	Model	Profits (￥1,000)	Average price (￥/h)	Fleet size	Average service rate (%)	Average number of relocations	Average number of access trips	Computation time (hours)
10	Integrated	236	78	976	87.45	812	677	3.80
	Separated	199	78	569	62.76	750	383	0.12
	Gap	-15.68%	0	-41.70%	-28.23%	-7.64%	-43.43%	-96.84
15	Integrated	236	78	975	87.21	816	671	5.75
	Separated	200	78	563	62.01	644	473	0.22
	Gap	-15.25%	0	-42.26%	-28.90%	-21.08%	-29.51%	-96.17%
30	Integrated	241	78	1,010	85.78	405	659	11.50
	Separated	205	78	569	61.55	321	448	0.53
	Gap	-15.10%	0	-43.66%	-28.25%	-20.63%	-32.01%	-95.39%

Results show that the optimization results obtained by the integrated approach outperform that obtained by the separated approach. The gaps in profits and fleet size between the two methods are as high as -15% and -28% respectively. The separated approach tends to maintain a smaller fleet size since the potential benefits from vehicle relocations are overlooked, leading to a large profit loss and service rate drop. On the other hand, it saves significant computation time by breaking the connection between the tactical and operational problems. The integrated method is more applicable for a median-scale network with around 50 zones and 1000 vehicles under demand uncertainty.

4.4.2 Comparative analysis between gradient search and other algorithms

We conduct the comparative analysis among 4 algorithms including Gurobi, GA, ILSA and GSA under 6 different scale instances with 1, 2, 3, 10, 15, 30 scenarios.

In Gurobi (Benchmark 1), we use default settings in solving **P0**. For ILSA (Benchmark 2), the step size of δ is set as 0.1 and 125 iterations are conducted. In GA (Benchmark 3), the iteration number is 8, population size is 10, chromosome length is 24, crossover rate is 0.8, and mutation rate is 0.005.

For small scale problems with 1, 2 or 3 demand scenarios, the global optimal solution can be obtained by solving **P0** via Gurobi directly. Hence, we only compare this global optimal solution with that by the proposed GSA. For cases with 4 or more scenarios, Gurobi had memory overflow. The cases with 10, 15 and 30 demand scenarios are tested by comparing the results among ILSA, GA and GSA. To the authors' best knowledge, the genetic, ant colony, simulated annealing and particle swarm optimization algorithms belong to random searching heuristic algorithms. They have the same disadvantage: only local optimal solution can be obtained and we are unable to quantify the solution quality. Hence, we introduce ILSA, which searches the neighborhoods of the local optimal solution obtained by GA and GSA. It works as a new benchmark algorithm. However, we have to acknowledge that the global optimal still cannot be guaranteed - unless no constraints on neighborhood boundary and search time. Table 8 shows the solution results.

Table 8 Comparative analysis of global and near global optimal solutions

Problem scale: No. of scenarios	Solution approaches	Profits (￥1,000)	Average price (￥/h)	Fleet size	Average service rate (%)	Average number of relocations	Average number of access trips	Computation time (seconds)
1	Gurobi	263	82	1,060	88.42	620	800	210
	GSA	260	82	1,051	88.67	746	686	5,380
	Gap	**-1.03%**	0	-0.85%	0.29%	20.32%	-14.25%	**2461.90%**
2	Gurobi	207	81	1,060	87.30	485	548	3,322
	GSA	205	82	1,051	87.39	447	527	6,846
	Gap	**-1.24%**	1.23%	-0.85%	0.10%	-7.94%	-3.92%	**106.08%**
3	Gurobi	211	81	1060	87.26	469	539	9,462
	GSA	208	81	1064	87.43	436	511	8,809

	Gap	**-1.53%**	0	0.38%	0.19%	-6.90%	-5.20%	**-6.90%**
10	ILSA	238	78	1,021	86.14	739	733	75,000
	GA	231	79	936	87.56	806	645	33,744
	GSA	236	78	976	87.45	812	677	13,680
	Gap between ILSA and GSA	**-0.84%**	0	-4.41%	1.52%	9.88%	-7.64%	**-81.76%**
	Gap between GA and GSA	**2.16%**	-1.27%	4.27%	-0.13%	0.74%	4.96%	**-59.46%**
15	ILSA	238	78	1,019	86.11	763	733	112,500
	GA	234	78	1,010	86.18	815	690	47643
	GSA	236	78	975	87.21	816	671	20,700
	Gap between ILSA and GSA	**-0.84%**	0	-4.32%	1.28%	6.95%	-8.46%	**-81.60%**
	Gap between GA and GSA	**0.85%**	0	-3.47%	1.20%	0.12%	-2.75%	**-56.55%**
30	ILSA	245	78	1,055	85.41	407	668	225,000
	GA	243	78	1,045	85.17	404	694	144,000
	GSA	241	78	1,010	85.78	405	659	41,400
	Gap between ILSA and GSA	**-1.63%**	0	-4.27%	0.43%	-0.49%	-1.35%	**-81.60%**
	Gap between GA and GSA	**-0.82%**	0	-3.35%	0.72%	0.25%	5.04%	**-71.25%**

For very small-scale problem with less than 3 scenarios, Gurobi is better in terms of both solution quality and computation time. However, 3 scenarios are far from representative. Those cases are presented here for illustration purpose only. For large-scale problem with over 3 scenarios, a better solution is obtained by using ILSA. Comparing to ILSA for the case of 30 scenarios, the GSA can obtain near optimal solutions with a optimality gap in profits less than 1.63%, yet grain as high as 81.6% savings in computation time. Comparing to GA, the GSA performs better in both solution quality and efficiency in most cases except the case of 10 scenarios. The differences in average price and profits are marginal. Overall, the solution quality obtained by GA and GSA algorithms is similar, but GA and ILSA needs a much longer computation time.

Further, we tested GA with four different population sizes: GA1 (ψ=4), GA2 (ψ=6), GA3 (ψ=8), GA4 (ψ=10). As shown in Table 9, a larger population size leads to a higher computation time (increases from 16 hours to 40 hours) yet a better solution quality (profit increases by 20%). One must find a tradeoff between the solution quality and computation time. Yet GA is unable to improve the solution quality further at a large population size. When we increase the population size from 8 (GA3) to 10 (GA4). the computation time increases significantly by 8 hours, yet the profit only increases by 1.6%. A better optimization result cannot be assured if increasing the population size further.

Table 9 Optimization results of the four GAs

Algorithms	Profits (￥1,000)	Average price (￥/h)	Fleet size	Average service rate (%)	Average number of relocations	Average number of access trips	Computation time (hours)
GA1	203	82	834	91.19	803	301	16
GA2	229	79	1,012	88.80	805	589	24
GA3	239	78	1,045	87.40	750	718	32
GA4	243	78	1,045	85.17	404	694	40

4.5 Remarks

According to the state-of-the-art studies in carsharing pricing, there are clear differences between trip pricing and user-based relocation strategies that both methods can be used to address the demand and supply imbalance problem. The trip pricing is used based on a demand-pricing elastic function that can estimate the maximum potential travel demand. The user-based relocation method can modify personal travel behavior including departure time and location with a given demand (Schiffer et al., 2021).

Normally, the carsharing operator offers payment discounts for user to conduct user-based relocations. The trip-joining and trip-splitting strategies (Barth et al., 2004; Uesugi et al., 2007), and trip-based or station-based discount strategies (Huang et al., 2020) are also used in user-based vehicle relocation operations. In this paper, we propose a new mode to address the vehicle supply shortage in operational level, which allows access trips by giving users allowances (access costs) together with staff-based relocations.

In this paper, the primary goal is to optimize the tactical decisions on fleet size and pricing. Based on the demand estimation on a particular day, vehicle relocations and access-trips are carried out to further balance the vehicle demand and supply. The user-based (allowing access trips) and operator-based (vehicle relocations) methods are used to handle the vehicle overflow and shortage under a particular demand scenario. In real-world operation, in case that demand estimation is only available in a few hours, we can take the tactical decisions as given and use the rolling horizon algorithm to optimize the number of relocations and access trips. This would ensure the absolute feasibility of the solutions while not overcomplicating the model. However, the shortcoming is that if future demand data of high accuracy is available, the rolling horizon method could lead to sub-optimal. Finally, in this paper, we do not use the rolling horizon method in case making this paper too long and complex.

5 Conclusion

This study developed a novel strategy that combines long-term prices, real-time relocations and access trips for the demand-supply imbalance problem under demand uncertainty. The carsharing vehicle fleet size and the price of trips are optimized in order to maximize the total profits of the operator by anticipating the vehicle relocations and access trips via walking or biking in the operational planning under uncertain demand. A two-stage stochastic programming is formulated on the basis of a service rate. A gradient search algorithm, a genetic algorithm and an iterated local search algorithm are proposed as a means to solve the program. To reduce computation time, parallel computing is used for solving different demand scenarios. A case study is conducted to demonstrate the applicability of the algorithms and to generate insights with respect to the management of one-way carsharing systems. The case study is based on a real traffic network in SIP in China and randomly generated demand formations from Poisson distributions.

The optimization results suggest that price of carsharing plays an important role in solving the long-term imbalance problem. A higher price reduces demand at high demand stations at peak hours, while maintaining profitability of the system. Considering the operational decisions for a typical day, real-time vehicle relocations in virtual relocation zones can reduce the imbalance problem. In addition, access trips in virtual access zones may further help to mitigate this problem since several clients can walk or cycle to the neighboring zones to pick-up vehicles. For the whole carsharing system, by using the pricing strategy, conducting real-time vehicle relocations, and allowing access trips, over 84% of all carsharing requests can be serviced.

Despite the fact that this research is already considering the flexible departure origins, it can still be improved by considering the full trip chain of clients. Clients may choose their pick-up or drop-off stations according to their activities. This can further improve the realism and the service level of the system. However, establishing a corresponding mathematical representation for such a problem is challenging. Moreover, to reduce the computational complexity, personnel movements are not considered in this paper. Another possible extension is to introduce rebalancing the staff to optimize the personnel movement routes and rebalance the drivers.

Acknowledgement

This research was financially supported by the Fundamental Research Funds for the Central Universities (No. 22120210111) at Tongji University.

References

An, K. (2014). Transit network design with stochastic demand. Doctoral dissertation. The Hong Kong University of Science and Technology.

An, K., & Lo, H. K. (2014). Ferry service network design with stochastic demand under user equilibrium flows. Transportation Research Part B, 66(8), 70-89.

An, K., & Lo, H. K. (2015). Robust transit network design with stochastic demand considering development density. Transportation Research Part B, 81, 737-754.

An, K., & Lo, H. K. (2016). Two-phase stochastic program for transit network design under demand uncertainty. Transportation Research Part B, 84, 157-181.

Balac, M., Becker, H., Ciari, F., & Axhausen, K. W. (2019). Modeling competing free-floating carsharing operators-A case study for Zurich, Switzerland. Transportation Research Part C, 98, 101-117.

Barrios, J. A., & Godier, J. D. (2014). Fleet sizing for flexible carsharing systems: Simulation-based approach. Transportation Research Record, 2416(1), 1-9.

Barth, M., Todd, M., & Xue, L. (2004). User-based vehicle relocation techniques for multiple-station shared-use vehicle systems. Transportation Research Record: Journal of the Transportation Research Board, 4161, 145-152.

Biondi, E., Boldrini, C., & Bruno, R. (2016). Optimal deployment of stations for a car sharing system with stochastic demands: a queueing theoretical perspective. In 2016 IEEE 19th International Conference on Intelligent Transportation Systems (ITSC), 1089-1095.

Boyacı, B., Zografos, K. G., & Geroliminis, N. (2015). An optimization framework for the development of efficient one-way car-sharing systems. European Journal of Operational Research, 240(3), 718-733.

Boyacı, B., Zografos, K. G., & Geroliminis, N. (2017). An integrated optimization-simulation framework for vehicle and personnel relocations of electric carsharing systems with reservations. Transportation Research Part B, 95, 214-237.

Boyacı, B., & Zografos, K. G. (2019). Investigating the effect of temporal and spatial flexibility on the performance of one-way electric carsharing systems. Transportation Research Part B, 129, 244-272.

Brandstätter, G., Kahr, M., & Leitner, M. (2017). Determining optimal locations for charging stations of electric car-sharing systems under stochastic demand. Transportation Research Part B, 104, 17-35.

Catalano, M., Lo Casto, B., & Migliore, M. (2008). Car sharing demand estimation and urban transport demand modelling using stated preference techniques.

Chen, Y., & An, K. (2021). Integrated optimization of bus bridging routes and timetables for rail disruptions. European Journal of Operational Research.

Ciari, F., Balac, M., & Balmer, M. (2015). Modelling the effect of different pricing schemes on free-floating carsharing travel demand: a test case for Zurich, Switzerland. Transportation, 42(3), 413-433.

Cocca, M., Giordano, D., Mellia, M., & Vassio, L. (2019). Free floating electric car sharing design: Data driven optimisation. Pervasive and Mobile Computing, 55, 59-75.

Correia, G. H., Jorge, D. R., & Antunes, D. M. (2014). The added value of accounting for users' flexibility and information on the potential of a station-based one-way car-sharing system: An application in Lisbon, Portugal. Journal of Intelligent Transportation Systems, 18(3), 299-308.

Dandl, F., & Bogenberger, K. (2018). Comparing future autonomous electric taxis with an existing free-floating carsharing system. IEEE Transactions on Intelligent Transportation Systems, 20(6), 2037-2047.

Di Febbraro, A., Sacco, N., & Saeednia, M. (2012). One-way carsharing: solving the relocation problem. Transportation research record, 2319(1), 113-120.

EVCARD, 2021.< https://www.evcard.com >(accessed: 2021-02-28).

Fan, W. D. (2014). Optimizing strategic allocation of vehicles for one-way car-sharing systems under demand uncertainty. In Journal of the Transportation Research Forum.

He, L., Hu, Z., & Zhang, M. (2020). Robust repositioning for vehicle sharing. Manufacturing & Service Operations Management, 22(2), 241-256.

He, L., Mak, H. Y., & Rong, Y. (2019). Operations management of vehicle sharing systems. Sharing Economy, 461-484.
He, L., Mak, H. Y., Rong, Y., & Shen, Z. J. M. (2017). Service region design for urban electric vehicle sharing systems. Manufacturing & Service Operations Management, 19(2), 309-327.
Heilig, M., Mallig, N., Schröder, O., Kagerbauer, M., & Vortisch, P. (2018). Implementation of free-floating and station-based carsharing in an agent-based travel demand model. Travel Behaviour and Society, 12, 151-158.
Herbawi, W., Knoll, M., Kaiser, M., & Gruel, W. (2016). An evolutionary algorithm for the vehicle relocation problem in free floating carsharing. In 2016 IEEE Congress on Evolutionary Computation, 2873-2879.
Huang, K., An, K., & Correia, G. H. (2020a). Planning Station Capacity and Fleet Size of One-way Electric Carsharing Systems with Continuous State of Charge Functions. European Journal of Operational Research. DOI: 10.1016/j.ejor.2020.05.001.
Huang, K., An, K., Rich. J., & Ma, W. (2020b). Vehicle relocation in one-way station-based electric carsharing systems: A comparative study of operator-based and user-based methods. Transportation Research Part E, 102081.
Huang, K., Correia, G. H., & An, K. (2018). Solving the station-based one-way carsharing network planning problem with relocations and non-linear demand. Transportation Research Part C, 90, 1-17.
Jorge, D., Molnar, G., & Correia, G. H. (2015). Trip pricing of one-way station-based carsharing networks with zone and time of day price variations. Transportation Research Part B, 81, 461-482.
Lee Y, Shariat S, Choi K. (2014). Optimizing skip-stop rail transit stopping strategy using a genetic algorithm. Journal of Public Transportation. 17(2): 135-164.
Li, X., Wang, C., & Huang, X. (2019). A Two-Stage Stochastic Programming Model for Car-Sharing Problem using Kernel Density Estimation. arXiv preprint arXiv:1909.09293.
Liu, Z., Meng, Q., & Wang, S. (2013). Speed-based toll design for cordon-based congestion pricing scheme. Transportation Research Part C, 31, 83-98.
Lu, M., Chen, Z., & Shen, S. (2018). Optimizing the profitability and quality of service in carshare systems under demand uncertainty. Manufacturing & Service Operations Management, 20(2), 162-180.
Lu, R., Correia, G. H. D. A., Zhao, X., Liang, X., & Lv, Y. (2020). Performance of one-way carsharing systems under combined strategy of pricing and relocations. Transportmetrica B: Transport Dynamics, 1-19.
Martínez, L. M., Correia, G. H., Moura, F., & Mendes Lopes, M. (2017). Insights into carsharing demand dynamics: Outputs of an agent-based model application to Lisbon, Portugal. International Journal of Sustainable Transportation, 11(2), 148-159.
Molnar, G., & Correia, G. H. (2019). Long-term vehicle reservations in one-way free-floating carsharing systems: A variable quality of service model. Transportation Research Part C, 98, 298-322.
Santos, G. G. D., & Correia, G. H. (2019). Finding the relevance of staff-based vehicle relocations in one-way carsharing systems through the use of a simulation-based optimization tool. Journal of Intelligent Transportation Systems, 1-22.
Schiffer, M., Hiermann, G., Rüdel, F., & Walther, G. (2021). A polynomial-time algorithm for user-based relocation in free-floating car sharing systems. Transportation Research Part B: Methodological, 143, 65-85.
Shaheen, S. A., & Cohen, A. P. (2013). Carsharing and personal vehicle services: worldwide market developments and emerging trends. International journal of sustainable transportation, 7(1), 5-34.
Shaheen, S. A., Cohen, A. P., & Roberts, J. D. (2006). Carsharing in North America: Market growth, current developments, and future potential. Transportation Research Record, 1986(1), 116-124.
SIP., 2017. <http://www.sipac.gov.cn/dept/wtjd/xwzx/201701/t20170119_524571.htm> (website accessed: 2019-10-10).
Vasconcelos, A. S., Martinez, L. M., Correia, G. H., Guimarães, D. C., & Farias, T. L. (2017). Environmental and financial impacts of adopting alternative vehicle technologies and relocation

strategies in station-based one-way carsharing: An application in the city of Lisbon, Portugal. Transportation Research Part D, 57, 350-362.
Xu, M., & Meng, Q. (2019). Fleet sizing for one-way electric carsharing services considering dynamic vehicle relocation and nonlinear charging profile. Transportation Research Part B, 128, 23-49.
Xu, M., Meng, Q., & Liu, Z. (2018). Electric vehicle fleet size and trip pricing for one-way carsharing services considering vehicle relocation and personnel assignment. Transportation Research Part B, 111, 60-82.
Uesugi, K., Mukai, N., & Watanabe, T. (2007). Optimization of vehicle assignment for car sharing system. In International Conference on Knowledge-Based and Intelligent Information and Engineering Systems, 1105-1111. Springer, Berlin, Heidelberg.
Wang, D.Z.W., Lo, H.K., 2008. Multi-fleet ferry service network design with passenger preferences for differential services. Transportation Research Part B, 42 (9), 798-822.
Wang, S., & Meng, Q. (2012). Sailing speed optimization for container ships in a liner shipping network. Transportation Research Part E, 48(3), 701-714.
Weikl, S., & Bogenberger, K. (2015). A practice-ready relocation model for free-floating carsharing systems with electric vehicles–Mesoscopic approach and field trial results. Transportation Research Part C, 57, 206-223.
Zheng, J., Scott, M., Rodriguez, M., Sierzchula, W., Platz, D., Guo, J. Y., & Adams, T. M. (2009). Carsharing in a university community: Assessing potential demand and distinct market characteristics. Transportation Research Record, 2110(1), 18-26.
Zhou, F., Zheng, Z., Whitehead, J., Perrons, R., Page, L., & Washington, S. (2017). Projected prevalence of car-sharing in four Asian-Pacific countries in 2030: What the experts think. Transportation Research Part C, 84, 158-177.

Appendix

Table A1 Optimization results in Stage-2

Scenario	Profits (￥)	Service rate (%)	Relocations	Access trips
1	240,999	87.20	464	709
2	244,509	86.18	371	711
3	238,521	85.12	396	614
4	239,256	85.15	375	584
5	240,392	86.64	432	688
6	239,540	85.25	395	639
7	242,232	86.53	402	712
8	242,505	86.77	448	699
9	239,326	86.12	391	646
10	238,786	84.53	419	565
11	239,774	83.92	362	603
12	242,181	86.38	377	678
13	241,464	86.60	396	704
14	239,407	87.39	454	684
15	241,240	85.15	461	632
16	238,819	83.83	389	592
17	243,219	85.92	389	693
18	241,793	86.33	390	709
19	243,266	87.03	440	673
20	239,921	84.34	408	639
21	237,930	85.30	390	645
22	240,150	84.55	374	643
23	233,889	85.37	408	630
24	242,684	85.96	404	678
25	240,921	86.94	436	688
26	240,006	83.74	376	621
27	242,129	84.52	401	619
28	242,861	86.39	398	709
29	239,015	87.35	428	660
30	240,649	86.77	382	691
Minimum value	233,889	83.74	362	565
Mean value	240,580	85.78	405	659
Maximum value	244,509	87.39	464	712
C.V	0.85%	1.27%	6.85%	6.33%